Inorg. Chem. **2005**, *44*, 4189–4205

Homoleptic, σ-Bonded Octahedral $[M(CO)_6]^{2+}$ Cations of Iron(II), Ruthenium(II), and Osmium(II): Part 1: Syntheses, Thermochemical and Vibrational Characterizations, and Molecular Structures as $[Sb_2F_{11}]^-$ and $[SbF_6]^-$ Salts. A Comprehensive, Comparative Study

Eduard Bernhardt,[†,‡,§] Christian Bach,[†] Bianca Bley,[†] Rudolf Wartchow,[†] Ulrich Westphal,[‡] Iona H. T. Sham,[||] Britta von Ahsen,[‡] Chanqing Wang,[||] Helge Willner,*[,†,‡,§] Robert C. Thompson,[||] and Friedhelm Aubke*[,||]

Institut für Anorganische Chemie der Universität Hannover, Callinstrasse 9, D-30167 Hannover, Germany, Fakultät 4, Anorganische Chemie, Gerhard Mercator Universität Duisburg, Lotharstrasse 1, D-47048 Duisburg, Germany, Department of Chemistry, The University of British Columbia, 2036 Main Mall, Vancouver B.C., V6T 1Z1 Canada, and FB C, Anorganische Chemie, Bergische Universität Wuppertal, Gaussstrasse 20, D-42097 Wuppertal, Germany

Received October 14, 2004

Homoleptic octahedral, superelectrophilic σ-bonded metal carbonyl cations of the type $[M(CO)_6]^{2+}$ (M = Ru, Os) are generated in the Brønsted–Lewis conjugate superacid HF/SbF_5 by reductive carbonylation of $M(SO_3F)_3$ (M = Ru, Os) or OsF_6. Thermally stable salts form with either $[Sb_2F_{11}]^-$ or $[SbF_6]^-$ as anion, just as for the previously reported $[Fe(CO)_6]^{2+}$ cation. The latter salts are generated by oxidative (XeF_2) carbonylation of $Fe(CO)_5$ in HF/SbF_5. A rationale for the two diverging synthetic approaches is provided. The thermal stabilities of $[M(CO)_6][SbF_6]_2$ salts, studied by DSC, range from 180 °C for M = Fe to 350 °C for M = Os before decarbonylation occurs. The two triads $[M(CO)_6][SbF_6]_2$ and $[M(CO)_6][Sb_2F_{11}]_2$ (M = Fe, Ru, Os) are extensively characterized by single-crystal X-ray diffraction and vibrational and ^{13}C NMR spectroscopy, aided by computational studies of the cations. The three $[M(CO)_6][SbF_6]_2$ salts (M = Fe, Ru, Os) crystallize in the tetragonal space group *P*4/*mnc* (No. 128), whereas the corresponding $[Sb_2F_{11}]^-$ salts are monoclinic, crystallizing in space group $P2_1/n$ (No. 14). In both triads, the unit cell parameters are nearly invariant of the metal. Bond parameters for the anions $[SbF_6]^-$ and $[Sb_2F_{11}]^-$ and their vibrational properties in the two triads are completely identical. In all six salts, the structural and vibrational properties of the $[M(CO)_6]^{2+}$ cations (M = Fe, Ru, Os) are independent of the counteranion and for the most part independent of M and nearly identical. Interionic C···F contacts are similarly weak in all six salts. Metal dependency is noted only in the ^{13}C NMR spectra, in the skeletal M–C vibrations, and to a much smaller extent in some of the C–O stretching fundamentals (A_{1g} and T_{1u}). The findings reported here are unprecedented among metal carbonyl cations and their salts.

Introduction

Mononuclear, homoleptic metal carbonyl complexes with regular octahedral coordination geometries, d^6 electron configurations, and diamagnetic $^1A_{1g}$ electronic ground states are known for 16 of the 24 transition metals that form thermally stable complexes with carbon monoxide. This large isostructural group of the general composition $[M(CO)_6]^m$ extends, as shown in Figure 1 together with their dates of discovery, from metal carbonyl anions ($m = 1-, 2-$) in groups 4 and 5[1,2] over the neutral, molecular metal carbonyls in group 6[3–5] and unipositive cations ($m = 1+$) in group

* To whom correspondence should be addressed. addressed. E-mail: willner@uni-wuppertal.de (H.W.).
† Institut für Anorganische Chemie der Universität Hannover.
‡ Gerhard Mercator Universität Duisburg.
§ Bergischen Universität Wuppertal.
|| The University of British Columbia.

(1) Ellis, J. E. *Adv. Organomet. Chem.* **1990**, *31*, 1.
(2) Ellis, J. E. *Organometallics* **2003**, *22*, 3322.
(3) Cotton, F. A.; Wilkinson, G. *Advanced Inorganic Chemistry*, 5th ed.; Wiley: New York, 1988.
(4) Elschenbroich, C.; Salzer, A. *Organometallics*, 2nd ed.; VCH: Weinheim, Germany, 1992.

10.1021/ic040115u CCC: $30.25
Published on Web 05/10/2005

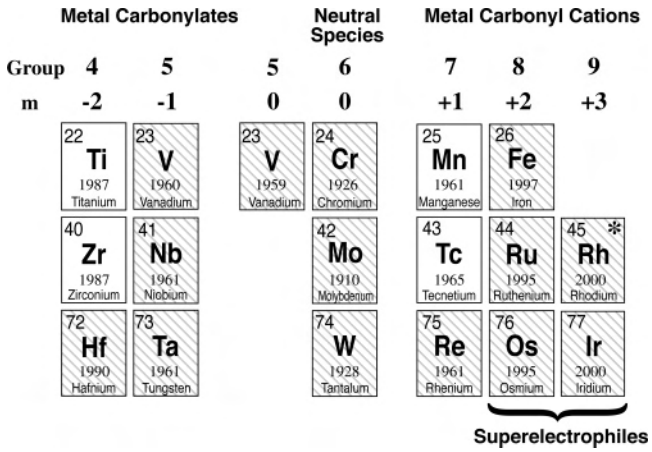

Figure 1. Transition metals that form octahedral homoleptic hexacarbonyls $[M(CO)_6]^m$. Shading indicates structurally characterized compounds. *$[Rh(CO)_5Cl]^{2+}$.

7[6,7] to the superelectrophilic,[8] predominantly σ-bonded metal carbonly cations[9−12] in groups 8 and 9 ($m = 2+, 3+$).

Whereas for groups 4−8 all members of a given triad are known (see Figure 1), for group 9 in $[Ir(CO)_6][SbF_6]_3 \cdot 4HF$,[13] a regular octahedral hexacarbonyl iridium(III) cation, is found. Rhodium(III) and iridium(III) form derivatives of the composition $[M(CO)_5Cl][Sb_2F_{11}]_2$ (M = Ir,[14,15] Rh[14,16]). The only homoleptic Co(I) carbonyl cation in $[Co(CO)_5][(CF_3)_3BF]$[17] has a trigonal-bipyramidal structure.

A larger number of homoleptic, octahedral metal carbonyl cations are found in group 8.[9−12] The reductive carbonylation of $M(SO_3F)_3$ (M = Ru, Os) in SbF_5 or HF/SbF_5 allows the isolation of $[M(CO)_6][Sb_2F_{11}]_2$ (M = Ru, Os).[18] Reductive carbonylation of OsF_6 in HF/SbF_5 provides a facile alternative route to $[Os(CO)_6][Sb_2F_{11}]_2$.[19] The cation $[Fe(CO)_6]^{2+}$(solv) is best obtained by oxidative carbonylation of $Fe(CO)_5$ in HF/SbF_5 with XeF_2 as an external oxidizer.[20] Single crystals of $[Fe(CO)_6][Sb_2F_{11}]_2$ are converted readily to $[Fe(CO)_6][SbF_6]_2$ by repeated washing with anhydrous HF. The molecular structures of both salts are reported, and all 13 vibrational fundamentals of $[Fe(CO)_6]^{2+}$ are observed.[20] Band positions and vibrational assignments together with structural parameters for $[Fe(CO)_6]^{2+}$ are confirmed by DFT calculations.[21]

There are four objectives of this study: (i) the syntheses and crystal growth of two sets of $[M(CO)_6]^{2+}$ salts (M = Ru, Os) with $[Sb_2F_{11}]^-$ and $[SbF_6]^-$ as the counter anions and subsequent molecular structure determination by single-crystal X-ray diffraction; (ii) a complete vibrational assignment of the $[M(CO)_6]^{2+}$ cations (M = Ru, Os) in analogy to the earlier study of the corresponding $[Fe(CO)_6]^{2+}$ salts,[20] supplemented by ^{13}C NMR data[9] and DFT calculations for $[M(CO)_6]^{2+}(g)$ (M = Fe, Ru, Os);[21,23] (iii) a thermal decomposition study supported by differential scanning calorimetry (DSC) measurements for $[M(CO)_6]^{2+}$ salts (M = Fe,[20] Ru, Os) with $[Sb_2F_{11}]^-$ or $[SbF_6]^-$; and (iv) the improvement and optimization of the reported[20] generation of $[Fe(CO)_6]^{2+}$(solv) by oxidative carbonylation of $Fe(CO)_5$ in HF/SbF_5.

The completion of this study and the inclusion of the results for the iron carbonyl fluoroantimonates[20] will permit an informed detailed "vertical" correlation of two triads of salts with $[M(CO)_6]^{2+}$ cations (M = Fe,[20] Ru, Os) and $[Sb_2F_{11}]^-$ or $[SbF_6]^-$ counteranions.

There have so far been a number of "horizontal" correlations, involving $[M(CO)_6]^m$ species (see Figure 1) mainly from the third (5d) transition series, based on both experimental[9,10,13,15] and computational[21−24] studies. Some results, relevant to this work,[9,10,13,15,21,23] are discussed below.

Experimental Section

General Procedures and Reagents. (a) Apparatus. Volatile materials were manipulated in a glass or stainless steel vacuum line of known volume equipped with a capacitance pressure gauge (type 280E, Setra Instruments, Acton, MA) and valves with PTFE stems (Young, London) or stainless steel needle valves (3762H46Y Hoke, Creskill, NJ), respectively. To remove moisture as $[H_3O][Sb_2F_{11}]$ in anhydrous HF, a small amount of SbF_5 was added, and the solutions were stored in a stainless steel cylinder or in PFA tubes (12 mm o.d., 300 mm long), heat gun sealed at the bottom and connected on top to a stainless steel needle valve (3762H46Y Hoke, Cresskil, NJ). All other volatile compounds were stored in glass containers equipped with a valve with a PTFE stem (Young, London). In the case of ^{13}CO, the storage vessel contained a molecular sieve (5 Å, Merck) to recover the excess of ^{13}CO after use by cooling with liquid nitrogen. For synthetic reactions in HF/SbF_5 solutions, a reactor was used consisting of a 120-mL PFA bulb with an NS 29 socket standard taper (Bohlender, Lauda, Germany) in connection with a PFA NS 29 cone standard taper and a PFA needle valve (Bohlender, Lauda, Germany). The two parts were pressed together with a metal flange, and the reactor was leak-tight ($<10^{-5}$ mbar L s^{-1}) without use of grease. A two-part V-shaped PFA vessel with valve was used to wash the product with anhydrous HF. Solid materials were manipulated inside an

(5) Crabtree, R. H. *The Organometallic Chemistry of the Transition Metals*, 2nd ed.; Wiley: New York, 1994.
(6) Abel, E. W.; Tyfield, S. P. *Adv. Organomet. Chem.* **1970**, *8*, 117.
(7) Beck, W.; Sünkel, K. *Chem. Rev.* **1988**, *88*, 1405.
(8) Olah, G. A. *Angew. Chem., Int. Ed. Engl.* **1993**, *32*, 167.
(9) Willner, H.; Aubke, F. *Angew. Chem., Int. Ed. Engl.* **1997**, *36*, 2402.
(10) Willner, H.; Aubke, F. *Organometallics* **2003**, *22*, 3612.
(11) Willner, H.; Aubke, F. In *Inorganic Chemistry Highlights*; Meyer, G. W., Naumann, D., Wesemann, L., Eds.; Wiley-VCH: Weinheim, Germany, 2002; p 195.
(12) Willner, H.; Aubke, F. *Chem. Eur. J.* **2003**, *9*, 1668.
(13) von Ahsen, B.; Berkei, M.; Henkel, G.; Willner, H.; Aubke, F. *J. Am. Chem. Soc.* **2002**, *124*, 8371.
(14) Willner, H.; Bach, C.; Wartchow, R.; Wang, C.; Rettig, S. J.; Trotter, J.; Jonas, V.; Thiel, W.; Aubke, F. *Inorg. Chem.* **2000**, *39*, 1933.
(15) Bach, C.; Willner, H.; Wang, C., Rettig, S. J.; Trotter, J.; Aubke, F. *Angew. Chem., Int. Ed. Engl.* **1996**, *35*, 1974.
(16) von Ahsen, B.; Berkei, M.; Köckerling, M.; Willner, H.; Hägele, G.; Aubke, F. *Inorg. Chem.* **2003**, *42*, 3801.
(17) Bernhardt, E.; Finze, M.; Willner, H.; Lehmann, C. W.; Aubke, F. *Angew. Chem., Int. Ed. Engl.* **2003**, *42*, 2077.
(18) Wang, C.; Bley, B.; Blazer-Jöllenbeck, G.; Lewis, A. R.; Siu, S. C.; Willner, H.; Aubke, F. *J. Chem. Soc., Chem. Commun.* **1995**, 2071.
(19) von Ahsen, B.; Bach, C.; Pernice, H.; Willner, H.; Aubke, F. *J. Fluorine Chem.* **2000**, *102*, 243.
(20) Bernhardt, E.; Bley, B.; Wartchow, R.; Willner, H.; Bill, E.; Kuhn, P.; Sham, I. H. T.; Bodenbinder, M.; Bröchler, R.; Aubke, F. *J. Am. Chem. Soc.* **1999**, *121*, 7188 and references therein.
(21) Jonas, V.; Thiel, W. *Organometallics* **1998**, *17*, 353.
(22) Szillagy, R. Frenking, G. *Organometallics* **1997**, *16*, 4807.
(23) Ehlers, A. W.; Ruiz-Morales, Y.; Baerends, F. J.; Ziegler, T. *Inorg. Chem.* **1997**, *36*, 5031.
(24) Diefenbach, A.; Bickelhaupt, F. M.; Frenking, G. *J. Am. Chem. Soc.* **2000**, *122*, 6449.

Table 1. Crystallographic Data for $[M(CO)_6][SbF_6]_2$ and $[M(CO)_6][Sb_2F_{11}]_2$ at 300 K (M = Fe,[20] Ru, Os)

	$[Fe(CO)_6][SbF_6]_2$	$[Ru(CO)_6][SbF_6]_2$	$[Os(CO)_6][SbF_6]_2$	$[Fe(CO)_6][Sb_2F_{11}]_2$	$[Ru(CO)_6][Sb_2F_{11}]_2$	$[Os(CO)_6][Sb_2F_{11}]_2$
emp formula	$C_6F_{22}FeO_6Sb_2$	$C_6F_{12}O_6RuSb_2$	$C_6F_{12}O_6OsSb_2$	$C_6F_{22}FeO_6Sb_4$	$C_6F_{22}RuO_6Sb_4$	$C_6F_{22}O_6OsSb_4$
formula weight	695.4	740.63	829.76	1128.9	1174.13	1263.26
cryst syst	tetragonal	tetragonal	tetragonal	monoclinic	monoclinic	monoclinic
space group	*P*4/*mnc* (No. 128)	*P*4/*mnc* (No. 128)	*P*4/*mnc* (No. 128)	$P2_1/n$ (No. 14)	$P2_1/n$ (No. 14)	$P2_1/n$ (No. 14)
color	colorless	colorless	colorless	colorless	colorless	colorless
a (Å)	8.258(1)	8.278(1)	8.274(1)	9.751(1)	9.798(1)	9.800(1)
b (Å)	8.258	8.278(1)	8.274(1)	12.457(1)	12.567(2)	12.544(1)
c (Å)	12.471(2)	12.449(2)	12.421(2)	10.542(1)	12.555(1)	10.536(1)
β (deg)	90	90	90	110.63(1)	110.78(1)	110.80(1)
V (Å^3)	850.5(2)	853.1(2)	850.3(2)	1198.4(2)	1215.1(3)	1210.8(2)
Z	2	2	2	2	2	2
GOF on F^2	1.03	1.058	1.001	0.843	1.01	1.15
R1 [$I > 2\sigma(I)$]	0.0259	0.0219	0.0196	0.0282	0.0330	0.0276
wR2	0.0668	0.0624	0.0506	0.0532	0.0692	0.0608

inert atmosphere box (Braun, Munich, Germany) filled with argon, with a residual moisture content of less than 1 ppm.

(b) Chemicals. Anhydrous HF and F_2 (Solvay AG, Hannover, Germany); Ru and Os (Degussa, Darmstadt, Germany); CO (99%, Linde Gas); HSO_3F, SO_3, and H_2SO_4 (Allied Chemicals); and ^{13}-CO (99% enriched, IC Chemicals) were obtained from commercial sources. Fluorosulfuric acid (technical grade) was purified by double distillation at room temperature as described previously.[25] Antimony(V) fluoride (Atochem North America, formerly Ozark-Mahoning) was purified by atmospheric pressure distillation, followed by vacuum distillation.[26] Bis(fluorosulfuryl)peroxide, $S_2O_6F_6$, was synthesized by catalytic (AgF_2) fluorination of SO_3 (Dupont) with elemental fluorine (Air Products) as described previously.[27,28]

The metal tris(fluorosulfates) $Ru(SO_3F)_3$[29] and $Os(SO_3F)_3$[30] were obtained by oxidation of the corresponding metals by $S_2O_6F_2$[27,28] in HSO_3F as described previously. OsF_6 was made by fluorination of Os as described earlier,[31] as was XeF_2 by fluorination of Xe.[32] $Fe(CO)_5$ (purity not stated, BASF, Ludwigshafen, Germany) was purified by trap-to-trap distillation.

(c) Instrumentation. (i) Vibrational Spectroscopy. Infrared spectra in the region 5000−400 cm^{-1} were recorded at room temperature on an IFS-66v FT spectrometer (Bruker, Karlsruhe, Germany) operating with a DTGS detector and a Ge/KBr beam splitter. Infrared spectra in the region 650−50 cm^{-1} were recorded at room temperature on an IFS-66v/s FT spectrometer with a DTGS detector and a Ge-coated 6-μm Mylar beam splitter (Bruker, Karlsruhe, Germany). One-hundred twenty-eight or 256 scans were co-added for each spectrum, using an apodized resolution of 2 or 4 cm^{-1}. The samples were crushed as Nujol mulls between AgBr (Korth, Kiel, Germany) or polyethylene (Cadillac, Hannover, Germany) disks inside the drybox.

Raman spectra were recorded at room temperature with a Bruker RFS 100/S FT Raman spectrometer using the 1064 nm exciting line (~500 mW) of a Nd:YAG laser (Adlas, DPY 301, Lübeck, Germany). For the correction of Raman intensities, a calibration tungsten lamp (3000 K) was used. Crystalline samples were contained in large melting point capillaries (2 mm o.d.) for recording spectra in the region 3500−80 cm^{-1} with a spectral resolution of 2 cm^{-1}. Two-hundred fifty-six or 128 scans were co-added for each spectrum.

(ii) NMR Spectroscopy. ^{13}C NMR spectra were obtained at room temperature on a Bruker DRX-500 FT spectrometer operating at 125.758 MHz. A 4-mm (o.d.) PFA tube, containing a saturated HF solution over solid $[M(^{13}CO)_6][SbF_6]_2$ (M = Ru, Os) was centered inside a 5-mm glass NMR tube containing the lock and external reference $CDCl_3$ (δ = 77.7 ppm referenced to TMS). The line width was 0.5−1.5 Hz. The ^{99}Ru and ^{187}Os satellites were detected.

(iii) Differential Scanning Calorimetry (DSC). Thermoanalytical measurements were made with a Netzsch DSC 204 instrument. Temperature and sensitivity calibrations in the temperature range of 20−600 °C were carried out with naphthalene, benzoic acid, KNO_3, $AgNO_3$, $LiNO_3$, and CsCl. The heating rate employed was 10 K min^{-1}, and the furnace was flushed with dry nitrogen. For the evaluation, the software Netzsch Proteus 4.0 was employed. The samples were contained in sealed stainless steel crucibles of an approximate mass of 1.3 g and a volume of 100 μL, which were coated on the inside with gold or rhodium (courtesy of Degussa-Hüls).

(iv) X-ray Diffraction. Under a dry argon atmosphere, fragments from single crystals of $[M(CO)_6][Sb_2F_{11}]_2$ and $[M(CO)_6][SbF_6]_2$ (M = Ru, Os) were cleaved and gently wedged into 0.3-mm capillary tubes with a trace of fluorocarbon grease as an adhesive. Data were recorded at room temperature with a Stoe IPDS diffractometer using graphite monochromatized Mo Kα radiation. The systematic absences observed for X-ray data of $[M(CO)_6][Sb_2F_{11}]_2$ (M = Ru, Os) uniquely defined the probable monoclinic space group to be $P2_1/n$, and those for $[M(CO)_6][SbF_6]_2$ (M = Ru, Os) point to two probable space groups, *P*4*nc* and *P*4/*mnc*, of which the latter centrosymmetric one was chosen on the basis of the successful crystal structure determinations. The structures were solved in $P2_1/n$ and *P*4/*mnc*, respectively, by direct methods (SHELXS-86),[33] and the final full-matrix least-squares refinements of all atomic parameters (SHELXL-93)[34] were carried out on a DECα Vax computer. The crystallographic data for $[Ru(CO)_6][Sb_2F_{11}]_2$, $[Os(CO)_6][Sb_2F_{11}]_2$, $[Ru(CO)_6][SbF_6]_2$, and $[Os(CO)_6][SbF_6]_2$ are summarized in Table 1.

(d) Synthetic Reactions. (i) Synthesis of $[M(CO)_6][Sb_2F_{11}]_2$ (M = Ru, Os). The PFA reactor described above, containing a PTFE-coated magnetic stirring bar, was charged with 0.40 g of $Ru(SO_3F)_3$ or 0.49 g of $Os(SO_3F)_3$ in a glovebox. To the reactor

(25) Barr, J.; Thompson, R. C.; Gillespie, R. J. *Inorg. Chem.* **1964**, *3*, 1149.
(26) Zhang, D.; Rettig, S. J.; Trotter, J.; Aubke, F. *Inorg. Chem.* **1996**, *35*, 6113.
(27) Dudley, F. B.; Cady, G. H. *J. Am. Chem. Soc.* **1959**, *79*, 513.
(28) Zhang, D.; Wang, C.; Mistry, F.; Powell, B.; Aubke, F. *J. Fluorine Chem.* **1996**, *76*, 83.
(29) Leung, P. C.; Aubke, F. *Can. J. Chem.* **1984**, *62*, 2892.
(30) Leung, P. C.; Wong, G. B.; Aubke, F. *J. Fluorine Chem.* **1987**, *35*, 607.
(31) Weinstock, B.; Malm, J. G. *J. Am. Chem. Soc.* **1958**, *80*, 4466.
(32) Holloway, J. H. *Chem. Commun.* **1966**, 22.
(33) Sheldrick, G. M. *SHELXS-86: Program for Crystal Structure Solution*; Universität Göttingen: Göttingen, Germany, 1986.
(34) Sheldrick, G. M. *SHELXS-93: Program for Crystal Structure Refinement*; Universität Göttingen: Göttingen, Germany, 1993.

were added 4 mL (55 mmol) of SbF_5 and 2 mL (100 mmol) of HF using a stainless steel vacuum line. At −196 °C, 9 mmol of CO was admitted to the reactor. The content was heated to 50−60 °C for 1−2 days without stirring, and colorless crystals of $[M(CO)_6][Sb_2F_{11}]_2$ (M = Ru, Os) formed. All volatile products were removed in vacuo. In the glovebox, the crystals were transferred into a V-shaped reactor. The crystalline product was washed with an SbF_5/HF (v/v 2:1) mixture. After removal of all volatiles in vacuo, 1.1 g (0.94 mmol, 94% yield) of pure $[Ru(CO)_6][Sb_2F_{11}]_2$ or 1.1 g (0.87 mmol, 87% yield) of pure $[Os(CO)_6][Sb_2F_{11}]_2$ was obtained. $[M(CO)_6][Sb_2F_{11}]_2$ salts (M = Ru, Os) were colorless moisture-sensitive crystalline solids. IR and Raman band positions and intensities attributed to the $[Sb_2F_{11}]^-$ anion in $[M(CO)_6][Sb_2F_{11}]_2$ (M = Ru, Os) were identical to those in $[Fe(CO)_6][Sb_2F_{11}]_2$.[20] Band positions and intensities attributed to the $[M(CO)_6]^{2+}$ cations in $[M(CO)_6][Sb_2F_{11}]_2$ (M = Ru, Os) were identical and very close to those in $[M(CO)_6][SbF_6]_2$, except for δCMC (ν_{11}) values, which were ca. 10 cm^{-1} lower. The isotopomers $[M(^{13}CO)_6][Sb_2F_{11}]_2$ (M = Ru, Os) were synthesized in an identical manner by using ^{13}CO.

(ii) Synthesis of $[M(CO)_6][SbF_6]_2$ (M = Ru, Os). Onto 1.1 g of powdered $[M(CO)_6][Sb_2F_{11}]_2$ (M = Ru, Os) contained in a "inverted-V" reactor made from PFA was condensed 2 mL of anhydrous HF in vacuo. The resulting suspension was stirred briefly, and the solid was allowed to settle. The supernatant solution was decanted into the sidearm. HF was recondensed into the main arm, and the washing process was repeated 7−10 times. After this washing, 0.66 g of $[Ru(CO)_6][SbF_6]_2$ and 0.69 g of $[Os(CO)_6][SbF_6]_2$ were obtained in crystalline form, which implied a yield of 95%. The $[M(CO)_6][SbF_6]_2$ salts (M = Ru, Os) were colorless moisture-sensitive crystalline solids. The isotopomers $[M(^{13}CO)_6][SbF_6]_2$ (M = Ru, Os) were obtained in an identical manner from $[M(^{13}CO)_6][Sb_2F_{11}]_2$ (M = Ru, Os). Band positions and intensities attributed to the $[SbF_6]^-$ anion in $[M(CO)_6][SbF_6]_2$ (M = Ru, Os) were identical to those in $[Fe(CO)_6][SbF_6]_2$.[20]

(iii) Synthesis of $[Os(CO)_6][Sb_2F_{11}]_2$ from OsF_6. Into a PFA flask of about 120 mL volume, fitted with a PFA top and a magnetic stirring bar, were added 2.3 g of SbF_5 and then 0.2 g of HF. With the mixture at liquid N_2 temperature, 0.13 g (0.43 mmol) of OsF_6 was added in vacuo. The CO pressure was then adjusted to give 1.5 atm at 25 °C. After being warmed to 40 °C, the mixture was stirred for 30 min. During this time, the solution turned from yellow to very pale yellow, and colorless crystal needles formed. Removal of all volatiles produced about 0.6 g of a purplish crystalline mass identified as $[Os(CO)_6][Sb_2F_{11}]_2$.

(iv) Preparation of $[Fe(CO)_6][Sb_2F_{11}]_2$ with XeF_2 as the Oxidizing Agent. In a typical experiment, 15 mL of HF, 1.52 g (9.1 mmol) of XeF_2, and 12 mL (160 mmol) of SbF_5 were condensed into a 250-mL PFA reactor. When a homogeneous solution had been obtained, 1.00 g (5.1 mmol) $Fe(CO)_5$ was added in vacuo at −196 °C. Then, 530 mbar (12 mmol) of CO was introduced into the system. The mixture was stirred at −50 °C in an ethanol bath for 10 min, and the color changed from white to yellowish. Stirring was then continued at 50 °C for 2 days. Upon removal of volatiles in vacuo, a mixture of white crystalline solid and powder was obtained and characterized by Raman spectroscopy. The crystalline products (5.62 g, expected 5.6 g) were isolated from the powder in the drybox. A portion of these crystalline solids was then washed with a (v/v 1: 1) mixture of HF and SbF_5 in a V-shaped PFA reactor to remove the powder on the surface of the crystals.

(v) Preparation of $[Fe(CO)_6][SbF_6]_2$ Obtained from the Reaction with XeF_2. Powdered $[Fe(CO)_6][Sb_2F_{11}]_2$ (4.625 g, 4.097 mmol, prepared as described above) was loaded into the main arm of a V-shaped PFA reactor. Five milliliters of HF was then added in vacuo. The resulting suspension was stirred briefly, and the crystals were allowed to settle. The supernatant solution was then decanted into the sidearm. Subsequently, HF was condensed back into the main arm. This washing process was repeated four times. After this washing, 3.905 g (5.6 mmol) of solids consisting of white powder and a few small white crystals was obtained in the main arm.

(vi) Improved Syntheses and Purification of $[Fe(CO)_6][Sb_2F_{11}]_2$ and $[Fe(CO)_6][SbF_6]_2$. The "crude" crystals of $[Fe(CO)_6][Sb_2F_{11}]_2$, prepared as described in (iv), were transferred to a 100-mL round-bottom PFA vessel, and subsequently 8 mL of HF and 1 bar of F_2 were introduced into the reactor. The mixture was stirred at room temperature for 2 days. Upon removal of volatiles, a white powder remained. This was identified as pure $[Fe(CO)_6][Sb_2F_{11}]_2$. An attempt to purify 3.9 g of the crude $[Fe(CO)_6][SbF_6]_2$ product was carried out by introducing 6 mL of HF and 1 bar of F_2 onto the solids in a round-bottom PFA flask. Pure $[Fe(CO)_6][Sb_2F_{11}]_2$ (2.672 g) in the form of a white powder was obtained upon removal of all volatiles. Some of the purified $[Fe(CO)_6][Sb_2F_{11}]_2$ (0.864 g, 0.765 mmol) was then converted back to $[Fe(CO)_6][SbF_6]_2$ (0.515 g, 0.741 mmol, 96.8% yield) by washing with HF.

Results and Discussion

(a) Synthetic Aspects. (i) General Comments. All presently known σ-bonded metal carbonyl cations[9−12] are either generated while dissolved in Brønsted or Brønsted−Lewis superacids[35,36] or obtained with the help of Lewis superacids.[37,38] The octahedral cations shown in Figure 1, found in groups 7−9,[6,7,9−12] are no exceptions. To generate the superelectrophilic[8] $[M(CO)_6]^{2+}$ cations (M = Fe,[20] Ru, Os) in group 8, the Lewis superacid SbF_5[37,38] and its solutions in HF to give the conjugate Brønsted−Lewis superacid HF/SbF_5,[39,40] are both suitable[9−12] and exclusively used.[18−20] In particular, HF/SbF_5 is a superb reaction medium that allows carbonlyation reactions to proceed in a homogeneous phase.[9−12]

There are four reasons for the use of HF/SbF_5 in the syntheses of salts with superelectrophilic[8] σ-bonded metal carbonyl cations: (i) Its excellent ionizing ability produces various cations by solvolysis, reduction or oxidation as reactive intermediates, that are easily carbonylated.[10−12] (ii) The final products are obtained in crystalline form, and a substantial number of accurate molecular structures have been determined recently by single-crystal X-ray diffraction.[10−12] (iii) Gaseous CO is moderately soluble in HF/SbF_5 and other superacids,[35,36] so that carbonylation reactions can proceed efficiently under very mild conditions (25−60 °C, $P_{CO} \sim 1$ atm). (iv) The superacid anions,[27] namely, $[Sb_2F_{11}]^-$ and $[SbF_6]^-$, are, according to ^{19}F NMR studies,[41] connected by equilibria of the type

$$[SbF_6]^-(solv) + SbF_5(solv) \overset{HF/SbF_5}{\rightleftharpoons} [Sb_2F_{11}]^-(solv) \quad (1)$$

In carbonylations, both anions will act as counteranions.

(35) O'Donnell, T. A. *Superacids and Acidic Melts as Inorganic Reaction Media*; VCH: Weinheim, Germany, 1993.
(36) Olah, G. A.; Prakash, G. K. S.; Sommer, J. *Superacids*; Wiley: New York, 1985.
(37) Fabré, P. L.; Devynk, J.; Tremillon, B. *Chem. Rev.* **1982**, *82*, 591.

Depending on the nature of the precursors used, three different synthetic routes are generally available,[9−12] with two of these used in the generation of $[M(CO)_6]^{2+}$ cations (M = Fe,[20] Ru, Os) in HF/SbF_5: (i) reductive carbonylation, where a high-valent metal compound of the type MX_m (X = F, Cl, SO_3F, etc.; $m = 3-6$) is reduced and carbonylated, with CO functioning as a reducing agent and ligand; (ii) oxidative methods, where low-valent metal carbonyls [Fe(CO)$_5$,[22] M(CO)$_6$;[41,42] M = Mo, W] or carbonyl derivatives {[Rh(CO)$_2$Cl]$_2$, [Ir(CO)$_3$Cl]$_x$}[14] are oxidized by either SbF_5 or an external oxidizer (AsF_5, Cl_2, XeF_2)[20] and carbonylated. The syntheses of the $[M(CO)_6]^{2+}$ salts (M = Fe,[20] Ru, Os) discussed below serve as illustrations for both synthetic pathways.

(ii) Generation and Isolation of Metal Carbonyl Fluoroantimonates (M = Ru, Os) by Reductive Carbonylation.[18] The synthesis of [M(CO)$_6$][Sb$_2$F$_{11}$]$_2$ (M = Ru, Os) by reductive carbonylation of M(SO_3F)$_3$ (M = Ru,[29] Os[30]) in HF/SbF_5 is formulated as:

$$2M(SO_3F)_3 + 16SbF_5 + 13CO \xrightarrow[50-60\ ^\circ C,\ 1-2\ days]{HF/SbF_5,\ 1\ atm\ CO} 2[M(CO)_6][Sb_2F_{11}]_2 + CO_2 + S_2O_5F_2 + 4Sb_2F_9(SO_3F) \quad (M = Ru, Os) \quad (2)$$

The reactions differ from the previous report,[18] where liquid SbF_5 was used as the reaction medium, on three accounts: (i) the reaction temperatures are lower by 10−30 °C and (ii) the reaction times are shorter by 1−2 days; however (iii) the isolated yields are no longer quantitative, being 94% for [Ru(CO)$_6$][Sb$_2$F$_{11}$]$_2$ and 79−87% for [Os(CO)$_6$][Sb$_2$F$_{11}$]$_2$.

Selected single crystals allow structure determinations and complete vibrational analyses for the $[M(CO)_6]^{2+}$ cations (M = Ru, Os). With no evidence of any side reactions or nonvolatile byproducts, the only cogent explanation is the presence of some $[SbF_6]^-$ as a counteranion, given that this anion and $[Sb_2F_{11}]^-$ are both present in HF/SbF_5[41] (see eq 1) and are both capable of stabilizing the $[M(CO)_6]^{2+}$ cations (M = Ru, Os). There is some evidence for this explanation: (a) A careful examination of the Raman spectra allows identification of the A_{1g} $[SbF_6]^-$ vibration at ∼650 cm^{-1}, and (b) the subsequent extrusion of SbF_5 by repeated washing of [M(CO)$_6$][Sb$_2$F$_{11}$]$_2$ (M = Ru, Os) with HF according to

$$[M(CO)_6][Sb_2F_{11}]_2 + 2HF \xrightarrow[50-60\ ^\circ C,\ 1-2\ days]{HF,\ 1\ atm\ CO} [M(CO)_6][SbF_6]_2 + 2HF/SbF_5 \quad (M = Ru, Os) \quad (3)$$

produces single crystals of pure [M(CO)$_6$][SbF_6]$_2$ (M = Ru, Os), but the reduction in bulk weight is only about 95% of that expected.

There is a precedent for the observed anion ambiguity: The reductive carbonylation of IrF_6 in SbF_5 or in concentrated solutions of SbF_5 in HF is reported to produce [Ir(CO)$_6$][Sb$_2$F$_{11}$]$_3$,[15,19] whereas in dilute HF/SbF_5 (6:1 by volume), [Ir(CO)$_6$][SbF_6]$_3$·4HF is formed and structurally characterized.[13] For both salts and for $[Ir(CO)_6]^{3+}$(solv),[15] band positions in the CO stretching region are all identical. In sharp contrast, formation of [M(CO)$_4$][Sb$_2$F$_{11}$]$_2$ (M = Pd, Pt),[43] [Hg(CO)$_2$][Sb$_2$F$_{11}$]$_2$,[44] and [Au(CO)$_2$][Sb$_2$F$_{11}$][45] by reductive[43,45] or solvolytic[44,45] carbonylation occurs in quantitative yields. In all instances, only $[Sb_2F_{11}]^-$ salts are known,[43−45] and only for gold is the structure of a salt formulated as [Au(CO)$_2$]$_2$[Sb$_2$F$_{11}$][SbF_6] reported.[46]

The reductive carbonylation of OsF_6 in HF/SbF_5[19] is a facile and fast alternative route to [Os(CO)$_6$][Sb$_2$F$_{11}$]$_2$. The four-electron reduction proceeds according to

$$OsF_6 + 8CO + 4SbF_5 \xrightarrow[HF/SbF_5,\ 1\ h]{40\ ^\circ C,\ 1.5\ atm\ CO} [Os(CO)_6][Sb_2F_{11}]_2 + 2COF_2 \quad (4)$$

However, despite the low reaction temperature and short reaction times, some purple color is noted, indicative of a further reduction of OsF_6. In addition, some $[SbF_6]^-$ appears to be present in the final product.

A useful rationale for the formation of fluoroantimonate salts of σ-bonded metal carbonyl cations[9−12] such as $[M(CO)_6]^{2+}$ (M = Ru, Os) in the strongly ionizing, conjugate Brønsted−Lewis superacid[35,36] HF/SbF_5[39,40] was introduced by us[12] recently: weakly solvated or "naked" metal cations such as Ru^{2+} or Os^{2+} (as well as Ir^{3+};[13] M^{2+}, M = Pd,[43] Pt, Hg,[44] or Au^+ [45]) are generated by reduction and/or solvolysis in the superacid matrix. They are viewed as soft or borderline Lewis acids, according to Pearsons soft and hard acid and base (SHAB) concept,[47] or as class b metal ions, according to an earlier classification by Ahrland, Chatt, and Davies,[48] and will react preferentially with the soft or b-class base CO(solv),[47,48] to form σ-bonded diamagnetic carbonyl cations with octahedral [M = Ir(III),[13] Ru(II), Os(II)], d^6 square-planar [M = Pd(II),[43] Pt(II)], d^8 linear [M = Hg(II),[44] Au(I)[45]], or d^{10} geometries. Isolable salts form with the superacid anions $[Sb_2F_{11}]^-$ [26] and $[SbF_6]^-$ in the case of octrahedral d^6 cations.[12]

The observed high thermal stabilities (vide infra) of the salts are attributed to three interrelated factors: (i) relativistic effects,[49,50] resulting in strong M−C bonds; (ii) extensive polarization of the C−O bond by the soft[47] or class b[48] M^{m+}

(38) Christe, K. O.; Dixon, D. A.; McLemore, D.; Wilson, W. W.; Sheehy, J. A.; Boatz, J. A. *J. Fluorine Chem.* **2000**, *101*, 151.
(39) Hyman, H. M.; Quaterman, L.; Kirkpatrick, M.; Katz, J. *J. Phys. Chem.* **1961**, *65*, 123.
(40) Gillespie, R. J.; Moss, K. C. *J. Chem. Soc. A* **1966**, 1170.
(41) Culman, J.-C.; Fauconet, M., Jost, R.; Sommer, J. *New J. Chem.* **1999**, *23*, 863 and references therein.
(42) Bröchler, R., Sham, I. H. T.; Bodenbinder, M.; Schmitz, V.; Rettig, S. J.; Trotter, J.; Willner, H.; Aubke, F. *Inorg. Chem.* **2000**, *39*, 2172.
(43) Willner, H.; Bodenbinder, M.; Bröchler, R.; Hwang, G.; Rettig, S. J.; Trotter, J.; v. Ahsen, B.; Westphal, U.; Jonas, V.; Thiel, W.; Aubke, F. *J. Am. Chem. Soc.* **2001**, *123*, 588.
(44) Bodenbinder, M.; Balzer-Jöllenbeck, G., Willner, H.; Batchelor, B. J.; Einstein, F. W. B.; Wang, C.; Aubke, F. *Inorg. Chem.* **1996**, *35*, 82.
(45) Willner, H.; Schaebs, J.; Hwang, G.; Mistry, F.; Jones, R.; Trotter, J.; Aubke, F. *J. Am. Chem. Soc.* **1992**, *114*, 8972.
(46) Küster, R.; Seppelt, K. *Z. Anorg. Allg. Chem.* **2000**, *626*, 236.
(47) Pearson, R. J. *J. Am. Chem. Soc.* **1963**, *85*, 3533.
(48) Ahrland, S.; Chatt, J.; Davies, N. R. *Q. Rev. Chem. Soc.* **1958**, *12*, 265.
(49) Pyykkö, P.; Desclaux, P. J. *Acc. Chem. Res.* **1979**, *12*, 276.
(50) Pyykkö, P. *Chem. Rev.* **1988**, *88*, 563.

acids, first discussed by Goldman and Krogh-Jesperson,[51] to explain the unusually high ν(CO) and f_{CO} values,[9−12] resulting in polar contributions to the M−C bonds; and (iii) the formation of extended molecular structures via significant interionic C···F interactions with the strongly electrophilic carbon atoms of the CO ligands in salts of superelectrophilic[8] σ-bonded metal carbonyl cations and the fluoroantimonate(V) anions.[10−12]

However, Fe^{2+}(solv) or other M^{2+}(solv) cations, formed mainly by metals in the 3d series, when generated in HF/SbF_5[39,40] or other superacids[35,36] in a similar manner, function as hard[47] or class a[48] acceptors toward $[SbF_6]^-$, resulting in the formation of layered materials of the type $M[SbF_6]_2$ with M = Cr, Mn, Fe, Co, Ni, Cu, Zn, Pd, Ag, Cd.[52] In these layered materials, the metal ions are octahedrally coordinated, frequently with paramagnetic ground states (except for the d^{10} ions).[53−55] Of the ions listed above, only Pd(II) can be carbonylated to give square-planar $[Pd(CO)_4]^{2+}$.[43]

In summary, the failure to generate $[Fe(CO)_6]^{2+}$(solv) by reductive carbonylation in HF/SbF_5 appears to be due to the acceptor characteristics of Fe^{2+},[47,48] and the difference in magnetic ground states of the MX_3 precursor (M = Fe, Ru, Os; X = Cl, SO_3F) as has been argued by us previously.[20] The synthesis of $[Fe(CO)_6]^{2+}$ salts by oxidation of $Fe(CO)_5$ by XeF_2 in HF/SbF_5 in the presence of CO(solv) provides an alternative approach, as discussed next.

(iii) Oxidative Carbonylation of $Fe(CO)_5$ by XeF_2 in HF/SbF_5 as the Reaction Medium. The recently[20] reported synthesis of $[Fe(CO)_6][Sb_2F_{11}]_2$ according to

$$Fe(CO)_5 + XeF_2 + CO + 4SbF_5 \xrightarrow[HF/SbF_5,\ 2\ days]{50\ °C,\ 1\ atm\ CO} [Fe(CO)_6][Sb_2F_{11}]_2 + Xe \quad (5)$$

appears to be straightforward and is a definite improvement over the reactions reported in our initial communication,[54] where SbF_5 had been used as reaction medium and Cl_2 or AsF_5 as the oxidizer. The reduced byproduct Xe(g) is now removed far more easily than found previously.[54] Crystalline $[Fe(CO)_6][SbF_6]_2$ is obtained by repeated washing with aHF, and molecular structures of both salts are determined by single-crystal X-ray diffraction.[20] The cation $[Fe(CO)_6]^{2+}$ is characterized by a complete vibrational analysis, including DFT calculations[21] and ^{13}C NMR and ^{57}Fe Mössbauer spectroscopies.[20] Detailed magnetic measurements allow an estimate of <0.1 mol % $Fe[SbF_6]_2$ as a paramagnetic impurity in the sample.

However, the final product, crystalline $[Fe(CO)_6][Sb_2F_{11}]_2$, is obtained in 50% yield only.[20] A recent careful analysis of the bulk material formed by evaporation of all volatiles[55] reveals a far greater complexity of the formation reaction than is suggested by eq 5. Details of this study,[55] in particular the magnetic properties, will be reported elsewhere.[56] The findings are briefly summarized here by listing additional components of the bulk reaction products.

The list includes the following species: (1) $[Fe(CO)_6][SbF_6]_2$ is found, which is not surprising in view of the findings for the corresponding $[M(CO)_6]^{2+}$ salts (M = Ru, Os) and the equilibrium (eq 1)[41] discussed above. (2) $Fe[SbF_6]_2$[52] is found in higher concentrations (~5 mol %) in the bulk. This material is nearly insoluble in HF/SbF_5 and can be separated by repeated recrystallization. A mechanism for its formation is proposed below. It is detected by bulk magnetic susceptibility measurements.[20,55,56] (3) $6SbF_3{\cdot}5SbF_5$ is detected by Raman spectroscopy.[57] Its composition is established by a crystallographic study.[61] This adduct is observed as reduced byproduct in the reported oxidation of $M(CO)_6$ (M = Mo,[58] W[42]) in HF/SbF_5 by SbF_5. Its presence in the bulk product mixture implies that SbF_5 functions as an oxidizer toward $Fe(CO)_5$, despite the fact that XeF_2 is used in excess (see Experimental Section). (4) $[XeF][Sb_2F_{11}]$[59,60] and similar adducts of XeF_2 and SbF_5 might explain why some XeF_2 might not act as an oxidizer (see eq 5). Its presence in the product mixture is suspected, but not clearly proven, because the diagnostic Xe−F stretching vibration, expected at 621 cm^{-1},[59,60] falls into an extremely cluttered region of the Raman spectrum.[52,55−57]

In summary, the complexity of the oxidative carbonylation of $Fe(CO)_5$ in HF/SbF_5 by XeF_2 is evident from the list discussed above, which might not be complete (vide infra). The list becomes even longer when AsF_5 or Cl_2 is used,[54] with the reduced byproducts far more difficult to remove[54] than Xe(g). Although careful recrystallization of the products avoids nearly all byproducts, the yield is reduced, and a rather simplistic view of the formation reaction results.

The previously reported[20] attempts to attack $[Fe(CO)_6]^{2+}$ salts with strong oxidizers (F_2, NiF_3) forms the basis for a useful purification method of crude $[Fe(CO)_6][Sb_2F_{11}]_2$, which involves the conversion of $6SbF_3{\cdot}5SbF_5$[61] into SbF_5 by fluorination with F_2 in aHF, according to

$$2(6SbF_3{\cdot}5SbF_5) + 12F_2 \xrightarrow[aHF,\ 2\ days]{25\ °C,\ 1\ atm\ F_2} 22SbF_5 \quad (6)$$

SbF_5 formed in this manner will also convert $[SbF_6]^-$ to $[Sb_2F_{11}]^-$ [41] according to

$$2SbF_5 + [Fe(CO)_6][SbF_6]_2 \xrightarrow[aHF,\ 2\ days]{25\ °C} [Fe(CO)_6][Sb_2F_{11}]_2 \quad (7)$$

and crude $[Fe(CO)_6][SbF_6]_2$ with a high $6SbF{\cdot}5SbF_5$[61] content is transformed to pure $[Fe(CO)_6][Sb_2F_{11}]_2$ by treat-

(51) Goldman, A. S.; Krogh-Jesperson, K. *J. Am. Chem. Soc.* **1996**, *118*, 12159.
(52) Gantar, D.; Leban, I.; Frlec, B.; Holloway, J. H. *J. Chem. Soc., Dalton Trans.* **1987**, 2379.
(53) Figgis, B. N. *Introduction to Ligand Fields*; Interscience: New York, 1966.
(54) Bley, B.; Willner, H.; Aubke, F. *Inorg. Chem.* **1997**, *36*, 158.
(55) Sham, I. H. T. Ph.D. Thesis, University of British Columbia, 2002.
(56) Sham, I. H. T.; Willner, H.; Thompson, R. C.; Aubke, F., manuscript in preparation.
(57) Birchall, T.; Dean, P. A. W.; Valle, B. D.; Gillespie, R. J. *Can. J. Chem.* **1975**, *53*, 667.
(58) Bröchler, R.; Freidank, D.; Bodenbinder, M.; Sham, I. H. T.; Willner, H.; Rettig, S. J.; Trotter, J.; Aubke, F. *Inorg. Chem.* **1999**, *38*, 3684.
(59) McRae, V. M.; Peacock, R. D.; Russel, D. R. *Chem. Commun.* **1969**, 62.
(60) Sladky, F. *Noble Gases*; Butterworth: London, 1972; Vol. 3.
(61) Nandana, W. A. S.; Passmore, J.; White, P. S. *J. Chem. Soc., Dalton Trans.* **1985**, 1623.

ment with F_2 in aHF at 25 °C. The purity of the iron carbonyl fluoroantimonate(V) salts is conveniently ascertained by Raman spectroscopy in the ν(Sb−F) region and comparison to published data.[20]

In summary, the complexity of the oxidative carbonylation of $Fe(CO)_5$, discussed here, and the simplicity of the reductive carbonylation of $M(SO_3F)_3$ (M = Ru,[29] Os[30]) or of OsF_6[19] with HF/SbF_5 as the reaction medium is apparent from two observations: (a) Even though $Ru(CO)_5$[62] and $Os(CO)_5$[63] have been known for 60 years[63] and longer[62] and more recent synthetic routes have been published,[64,65] their use in oxidations and carbonylations is impractical and unnecessary. Their molecular structures,[66,67] however, obtained by electron diffraction, allow useful comparisons to the $[M(CO)_6]^{2+}$ cation (M = Ru, Os) reported here. (b) $[Fe(CO)_6]^{2+}$, reported here and elsewhere,[20,54] is thus far the only known homoleptic metal carbonyl cation obtained by oxidative carbonylation.[9−12] Early claims of its synthesis by halide abstraction from $M(CO)_4X_2$ (M = Fe, Os) with $M'X_3$ (M′ = Al, Fe; X = Cl, Br) at high T and p_{CO}[68] or by amine-catalyzed disproportionation of $Fe(CO)_5$[69] have been either retracted[70] or discredited.[6,7]

There is another interesting, albeit erroneous, connection between $[Fe(CO)_6]^{2+}$ [54] and $[Os(CO)_6]^{2+}$ [18] based on preliminary findings: observations of weak IR bands in the CO stretching region, at 2256 cm^{-1} for the $[Fe(CO)_6]^{2+}$ ion and at 2252 cm^{-1} for $[Os(CO)_6]^{2+}$, had suggested the presence of small amounts of $[M(CO)_6]^{3+}$ (M = Fe, Os), given that the IR-active fundamental ν_6 (T_{1u}) for $[Ir(CO)_6]^{3+}$ is found at 2254 cm^{-1}.[13,15,19] Upon reinvestigation, the two bands in question are now attributed to the cations $[ClCO]^+$ [71] and *trans*-$[O_2Os(CO)_4]^{2+}$,[72] respectively.

(iv) Thermal Stabilities of Metal Carbonyl Fluoroantimonates (M = Fe, Ru, Os). Thermal stabilities and decomposition pathways of $[Fe(CO)_6][Sb_2F_{11}]_2$ and $[M(CO)_6][SbF_6]_2$ (M = Fe, Ru, Os) were studied by DSC (differential scanning calorimetry). The corrosive nature of the decomposition products limits the studies to the determination of the onset temperatures and a description of peak shapes of thermal events. To allow the interpretation of these events, DSC measurements were preceded by heating small samples in glass vials. Gaseous products were identified by IR spectroscopy, and solid residues were studied by Raman spectroscopy. A similar DSC study of the related salts $[M(CO)_4][Sb_2F_{11}]_2$ (M = Pd, Pt)[43] has been published.

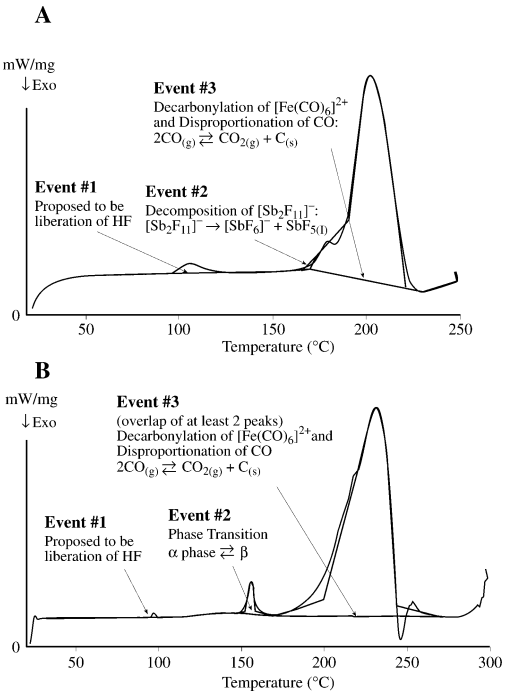

Figure 2. DSC plots in the temperature range of 25−300 °C of (A) $[Fe(CO)_6][Sb_2F_{11}]_2$ and (B) $[Fe(CO)_6][SbF_6]_2$.

The Fe(II) salts $[Fe(CO)_6][Sb_2F_{11}]_2$ and $[Fe(CO)_6][SbF_6]_2$[20,54,55] are the main focus of this study for two reasons: (i) The principal decarbonylation products, paramagnetic $Fe[SbF_6]_2$[52] and FeF_2, obtained at T > 400 °C, are more clearly defined than those of $[M(CO)_6][SbF_6]_2$ (M = Ru, Os). (ii) In HF/SbF_5, only mixed $[Sb_2F_{11}]^-$ and $[SbF_6]^-$ salts of $[M(CO)_6]^{2+}$ (M = Ru, Os) are obtained, which are converted to pure $[M(CO)_6][SbF_6]_2$ (M = Ru, Os) as described and studied here by DSC.

The DSC plot of $[Fe(CO)_6][Sb_2F_{11}]_2$ and $[Fe(CO)_6][SbF_6]_2$ in the temperature range of 25−300 °C is shown in Figure 2. There are four endothermic events: (i) A small, irreversible peak at ∼100 °C in both salts appears to be due to the evolution of small amounts of HF, presumably present in samples prepared in HF. (ii) A reversible event, attributed to a phase transition, is found for all three $[M(CO)_6][SbF_6]_2$ salts, at 151 °C for the Fe compound, at 163 °C for the Ru compound, and at 173 °C for the Os compound. A possible explanation is a change in orientation of the octahedral ions in the lattice upon heating and possibly even a transition from tetragonal to cubic symmetry. (iii) Elimination of SbF_5 from $[Fe(CO)_6][Sb_2F_{11}]_2$ gives rise to an endothermic shoulder at 170 °C. SbF_5 and $[Fe(CO)_6][SbF_6]_2$ as residues are identified by their Raman spectra. For $[M(CO)_6][Sb_2F_{11}]_2$ (M = Ru, Os), sample shrinking at ∼170 °C was reported in a preliminary communication[18] and is probably due to the loss of SbF_5. (iv) Broad, strongly endothermic peaks due to the simultaneous, irreversible loss of all six CO ligands are found for the four salts with the follwing onset temperatures: $[Fe(CO)_6][Sb_2F_{11}]_2$, 185 °C; $[Fe(CO)_6][SbF_6]_2$, 180 °C; $[Ru(CO)_6][SbF_6]_2$, 280 °C; and $[Os(CO)_6][SbF_6]_2$, 350 °C. Volatile CO(g) and CO_2(g) are detected by IR spectros-

(62) Manchot, W.; Manchot, W. J. *Z. Anorg. Allg. Chem.* **1936**, *236*, 385.
(63) Hieber, W.; Stallmann, H. *Z. Elektrochem.* **1943**, *49*, 288.
(64) Calderazzo, F.; L'Eplattenier, F. *Inorg. Chem.* **1967**, *6*, 1220.
(65) Rushman, P.; van Buren, G. N.; Shiralian, M.; Pomeroy, R. K. *Organometallics* **1983**, *2*, 693.
(66) Huang, J.; Hedberg, K.; Pomeroy, R. K. *Organometallics* **1988**, *7*, 2049.
(67) Huang, J.; Hedberg, K.; Davies, H. B.; Pomeroy, R. K. *Inorg. Chem.* **1990**, *29*, 3923.
(68) Hieber, W.; Kruck, T. *Angew. Chem.* **1961**, *73*, 580.
(69) Sternberg, H. W.; Friedel, A. R.; Shufler, S. L.; Wender, I. J. *J. Am. Chem. Soc.* **1955**, *77*, 2675.
(70) Hieber, W.; Frey, V.; John, P. *Chem. Ber.* **1967**, *100*, 1961.
(71) Bernhardt, E.; Willner, H.; Aubke, F. *Angew. Chem., Int. Ed.* **1999**, *36*, 823.
(72) Bernhardt, E.; Willner, H.; Jonas, V.; Thiel, W.; Aubke, F. *Angew. Chem., Int. Ed.* **2000**, *39*, 168.

copy. In addition, a black coating is observed at this stage, which is explained by the equilibrium[55,56]

$$2CO \rightleftarrows CO_2 + C \qquad (8)$$

The results of a previous DSC study of $[M(CO)_4][Sb_2F_{11}]_2$ (M = Pd, Pt[43]) differ on two accounts: (i) Evolution of SbF_5 does not occur, and no evidence for the existence of $[M(CO)_4][SbF_6]_2$ is obtained. (ii) Complete loss of CO is evident from broad, single peaks with onsets at 180 (Pd) and 230 °C (Pt), but only COF_2 is found in the gas phase, together with CO_2 and SiF_4, indicative of some partial hydrolysis. The demonstrated involvement of $[Sb_2F_{11}]^-$ in extended structure formation with significant C···F contacts provides an explanation for both observations.

The complete, irreversible loss of all CO ligands upon heating, with decomposition well above 150 °C, is a characteristic feature of fluoroantimonate salts with σ-bonded metal carbonyl cations.[9−12] Thus far, no evidence has been found for the existence of metal carbonyl cations with a low CO content, formed by the controlled pyrolysis of existing, thermodynamically stable metal carbonyl cations.[9−12]

Stepwise reversible dissociation of CO at room temperature is found only for thermally unstable polycarbonyl complexes of Ag(I) and Cu(I),[73−75] called "non-classical carbonyls",[75] which are formed by stepwise, reversible addition of up to four CO molecules to silver(I) and copper(I) salts with weakly coordinating anions.[76−78] This contrasting thermal behavior reflects a weak, dative OC → M bond (M = Ag, Cu), the absence of relativistic contributions[49,50] to the M−CO bond, and ineffective bond polarization[51] by Ag(I) and Cu(I), as discussed recently.[10,12]

(v) Oxidative Carbonylation of $Fe(CO)_5$ in Superacids: Mechanism and Rationale. Two observations mark the outset of our discussion on mechanistic aspects. (i) From detailed magnetic susceptibility studies,[20,55,56] it is clear that all preparations of $[Fe(CO)_6][Sb_2F_{11}]_2$ will contain variable amounts of a paramagnetic impurity, identified as $Fe[SbF_6]_2$.[52] Its actual content can be as high as 38−32 mol % when Cl_2 or AsF_5 is used as the oxidizer in SbF_5 or as low as 0.4% with XeF_2 in HF/SbF_5.[20] Conversion to crystalline $[Fe(CO)_6][SbF_6]_2$ by repeated washing with aHF reduces the $Fe[SbF_6]$ content to about 0.1 mol %.[20,55] (ii) From the DSC study discussed above (Figure 2), it is apparent that temperatures well in excess of 170 °C are required to thermolyse $[Fe(CO)_6][Sb_2F_{11}]_2$[20] to $Fe[SbF_6]_2$.[52] As discussed in the section on synthesis, the temperatures required for reaction and product isolation are 50 °C or lower (see eq 5). These observations allow two conclusions to be drawn: (a) $Fe[SbF_6]_2$,[52] found as an impurity, is very likely not a decomposition product of $[Fe(CO)_6][Sb_2F_{11}]_2$ or $[Fe(CO)_6][SbF_6]_2$ but rather a byproduct, formed during the reductive carbonylation of $Fe(CO)_5$.[20,54−56] (b) Formation of $Fe[SbF_6]_2$ appears to be strongly dependent on the reaction medium and the oxidizing agents employed. A summary of the proposed oxidation, carbonylation, and salt formation reactions is shown for both SbF_5 and HF/SbF_5 in Scheme 1.

Scheme 1

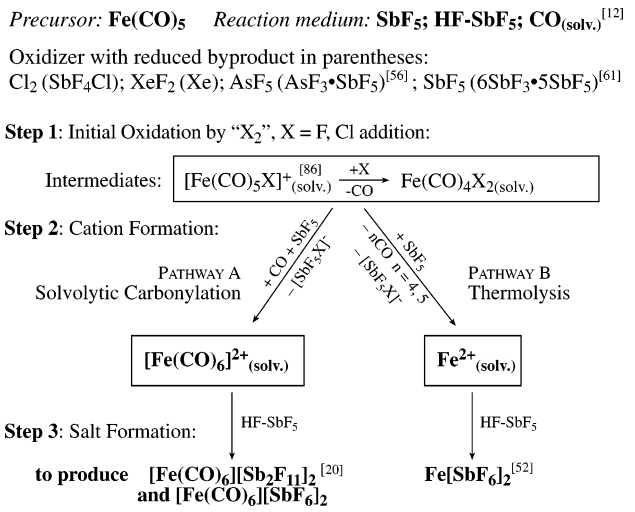

The initial process in the oxidative carbonylation is formally a two-electron oxidative addition of two halogens to $Fe(CO)_5$, dissolved or suspended in HF/SbF_5 or SbF_5. The halogens are provided by the oxidizing agent Cl_2;[54] XeF_2;[20,55] or EF_5,[54] E = As, Sb.[55]

Early synthetic studies by W. Hieber[79] and students[80−82] discovered the *partial oxidative substitution* reactions

$$Fe(CO)_5 + X_2 \rightarrow Fe(CO)_4X_2 + CO \qquad X = I, Br, Cl \qquad (9)$$

The thermal stabilities of the products decrease with increasing electronegativity of X and it is not surprising that $Fe(CO)_4F_2$ has not yet been isolated.[83,84] Thermal decomposition involves complete or partial loss of CO [i.e., the existence of $Fe(CO)_2Cl_2$ is claimed[79,85]].

In addition, at low temperature[80] or in liquid HCl,[86] an intermediate of the type $Fe(CO)_5Cl_2$ is obtained *by oxidative addition* and stabilized by addition of BCl_3 as $[Fe(CO)_5Cl][BCl_4]$, which decomposes at 25 °C under evolution of BCl_3.[86]

On the basis of these precedents, the existence of two species in HF/SbF_5 or SbF_5 is anticipated: the cation $[Fe(CO)_5X]^+$(solv) or the neutral species $Fe(CO)_4X_2$ (X = Cl, F), with the fluoro species as reactive transients. Two competing reactions are possible: (i) Solvolytic carbonylation[10−12] is expected to convert either $[Fe(CO)_5X]^+$ or $Fe(CO)_4X_2$ (X = Cl, F) into $[Fe(CO)_6]^{2+}$(solv). This step

(73) Hurlburt, P. K.; Rack, J. J.; Luck, J. S.; Dec, S. F.; Webb, J. D.; Anderson, O. P.; Strauss, S. H. *J. Am. Chem. Soc.* **1994**, *116*, 10003.
(74) Strauss, S. H. *J. Chem. Soc., Dalton Trans.* **2000**, 1.
(75) Lupinetti, A. J.; Frenking, G.; Strauss, S. H. *Prog. Inorg. Chem.* **2001**, *49*, 1.
(76) Krossing, I. *Chem. Eur. J.* **2001**, *7*, 490.
(77) Reed, C. *Acc. Chem. Res.* **1998**, *31*, 133.
(78) Strauss, S. H. *Chem. Rev.* **1993**, *93*, 927.
(79) Hieber, W. *Advances in Organometallic Chemistry*; Academic Press: New York, 1970; Vol. 8.
(80) Hieber, W.; Bader, C. *Chem. Ber.* **1928**, *61*, 1717.
(81) Hieber, W.; Lagally, H. *Z. Anorg. Allg. Chem.* **1940**, *245*, 295.
(82) Hieber, W.; Wirsching, A. *Z. Anorg. Allg. Chem.* **1940**, *245*, 35.
(83) Doherty, N. N.; Hoffman, N. W. *Chem. Rev.* **1991**, *91*, 553.
(84) Murphy, E. F.; Murgavel, R.; Roesky, H. W. *Chem. Rev.* **1997**, *97*, 3425.
(85) Hieber, W.; Lagally, H.; Wirsching, A. *Z. Anorg. Allg. Chem.* **1940**, *245*, 3005.
(86) Iqbal, Z.; Waddington, T. C. *J. Chem. Soc. A* **1968**, 1238.

involves formation of the transient 14- or 16-electron cations $[Fe(CO)_m]^{2+}$(solv) ($m = 4, 5$), which act as soft[47] or class b[48] acceptors. They are readily converted by reaction with the soft[47] donor CO to the stable 18-electron cation $[Fe(CO)_6]^{2+}$(solv). This step is facilitated in an ionizing solvent such as HF/SbF_5,[39−41] which provides the superacid anions $[Sb_2F_{11}]^-$ and $[SbF_6]^-$ [26,41] as counteranions. A precedent for the overall process is the recently reported solvolytic carbonylation of $[Rh(CO)_2(\mu\text{-}Cl)]_2$ into $[Rh(CO)_4]^+$(solv) in HSO_3F,[16] (ii) Thermal decarbonylation, as observed for solid $Fe(CO)_4Cl_2$,[79,82] is seen as a competing process that provides a facile pathway to $Fe[SbF_6]_2$[52] via Fe^{2+}(solv) functioning[10,12] as hard[47] or class b[48] acceptor toward the hard base $[SbF_6]^-$.[47,48] This alternate pathway is facilitated in SbF_5, where higher reaction temperatures (up to 90 °C),[54] needed to reduce the viscosity of SbF_5,[9] and longer reaction times[54] are conducive to thermolysis as a side reaction.

In summary, although the conditions that favor formation of $[Fe(CO)_6]^{2+}$ in very high yields[20,55] are clearly outlined in this section—HF/SbF_5[39−41] as the reaction medium, XeF_2 as the oxidizer,[20,55] resulting in low reaction temperatures and short reaction times and product purification by careful recrystallization[20]—it has thus far not been possible to completely eliminate the formation of $Fe[SbF_6]_2$ in competing side reactions. Our inability to synthesize diamagnetic $[Fe(CO)_6]^{2+}$ salts does not rule out an alternative interpretation that the weak paramagnetism observed is due to TIP (temperature-independent paramagnetism).[53]

(vi) Synthetic Aspects: Summary and Conclusion. The reductive carbonylation of $M(SO_3F)_3$[29,30] (M = Ru, Os) or of OsF_6[31] in HF/SbF_5[39−41] described here allows the generation of the octahedral cations $[M(CO)_6]^{2+}$(solv) (M = Ru, Os)[18,19] and the subsequent isolation of two sets of crystalline salts with either $[Sb_2F_{11}]^-$ or $[SbF_6]^-$ as counteranions in quantitative yields and very high purities. A previously proposed[10,12] rationale for the formation of $[M(CO)_6]^{2+}$ cations (M = Ru, Os), based on the solubility of CO in SbF_5[87] and HF/SbF_5[10,12,87] and soft[47] or class b[48] acceptor properties of the naked M^{2+}(solv) cation (M = Ru, Os),[10,12] is adopted for both group 8 cations, and the formation of two types of salts is explained by the well-known solution equilibrium in HF/SbF_5.[41]

In sharp contrast, the previously reported[20,54] salts $[Fe(CO)_6][Sb_2F_{11}]_2$ and $[Fe(CO)_6][SbF_6]_2$ can be obtained only by oxidative carbonylation of $Fe(CO)_5$, although the formation reactions in HF/SbF_5 with XeF_2 as the oxidizer are much more complex, as discussed.[20,55] Small amounts of paramagnetic $Fe[SbF_6]_2$[52] remain in samples prepared under optimal conditions—oxidation of $Fe(CO)_5$ by XeF_2 in HF/SbF_5[38−41] at 25 °C—even after careful recrystallization.[20,55] A rationale is proposed, again based on the SHAB concept[47] and the metal ion classification by Ahrland, Chatt, and Davies,[48] for the formation of both $[Fe(CO)_6][Sb_2F_{11}]_2$[20] and $Fe[SbF_6]_2$[52] by two competing pathways: solvolytic carbonylation following oxidation to transient $[Fe(CO)_m]^{2+}$ ($m = 4, 5$) and thermolysis of intermediates to Fe^{2+}(solv). The crystal, molecular, and extended molecular structures of all six salts are discussed in the next section.

(b) Structural Aspects. (i) General Comments. As is evident from the selected crystallographic data collected in Tables 1 and 2 and the more extensive listings provided as Supporting Information in Tables S1 and S2, the two previously characterized $[Fe(CO)_6]^{2+}$ salts[20] and the four metal carbonyl fluoroantimonates (M = Ru, Os; see Table 1) form two isostructural triads with very similar unit cell dimensions. Within each triad, the $[Sb_2F_{11}]^-$ salts crystallize in the monoclinic space group $P2_1/n$ (No. 14), whereas the three $[SbF_6]^-$ compounds have tetragonal structures with the space group $P4/nmc$ (No. 128).

Among superelectrophilic,[8] structurally characterized σ-bonded, cationic metal carbonyl compounds,[9−11] isostructural pairs have previously been reported for octahedral $[M(CO)_5Cl][Sb_2F_{11}]_2$ (M = Rh, Ir)[13] and square-planar $[M(CO)_4][Sb_2F_{11}]_2$ (M = Pd, Pt).[43] In these monoclinic pairs, very similar unit cell parameters are found,[13,43] with the 5d complexes (Ir^{III}, Pt^{II}) having slightly smaller unit cell volumes than their 4d (Rh^{III}, Pd^{II}) congeners. This is attributed to relativistic effects.[49,50] As a consequence, similar structural and spectrosopic properties for the two cations of each pair[13,43] are observed. However, the $[Sb_2F_{11}]^-$ counteranions in each pair are not symmetry related, and important diagnostic parameters for the two anions differ markedly.[13,43] As a consequence, in each of the two pairs, there are a total of four crystallographically different $[Sb_2F_{11}]^-$ anions. This results in differences in the observed significant interionic contacts[14,43] to form extended structures. For a third isostructural pair, the square-planar molecular complexes *cis*-$M(CO)_2(SO_3F)_2$[88,89] (M = Pt, Pd), the two sets of structural and spectroscopic parameters differ measurably.

The two triads of $[M(CO)_6]^{2+}$ complexes (M = Fe,[20] Ru, Os) discussed here and previously[20] include in the comparison with $[Fe(CO)_6]^{2+}$ the only known superelectrophilic σ-bonded metal carbonyl cation[9−12] formed by a 3d metal. In addition, two different symmetry-related anions,[20] $[Sb_2F_{11}]^-$ and less common $[SbF_6]^-$,[9−12] permit us to probe both the metal and anion dependencies of structural and spectroscopic data. All of these data were obtained in our laboratories using nearly identical instrumentation and physical methods (see Experimental Section here and in ref 20).

Therefore, rather than presenting and discussing experimental and relevant computational[21−24] data for the metal carbonyl fluoroantimonates for M = Ru and Os in isolation and in a similar manner as reported for isostructural $[Fe(CO)_6][Sb_2F_{11}]_2$ and $[Fe(CO)_6][SbF_6]_2$,[20] we intend to compare all six salts in this study with three basic objectives: (i) to explore the extent to which the crystal data for the salts, the bond parameters (internuclear distances and bond angles) for both the $[M(CO)_6]^{2+}$ cations (M = Fe,[20] Ru, Os) and the two fluoroantimonate anions $[Sb_2F_{11}]^-$ and $[SbF_6]^-$,

(87) von Ahsen, B.; Bley, B.; Bodenbinder, M.; Balzer, G.; Willner, H.; Hwang-Mistry, G.; Wang, C.; Hägele, G.; Aubke, F. *Inorg. Chem.*, in preparation.

(88) Wang, C.; Willner, H.; Bodenbinder, M.; Batchelor, R.; Einstein, F. W. B.; Aubke, F. *Inorg. Chem.* **1994**, *33*, 3521.

(89) von Ahsen, B.; Wartchow, R.; Willner, H.; Jonas, V.; Aubke, F. *Inorg. Chem.* **2000**, *39*, 4424.

Table 2. Crystallographic and Structural Data for Various Structure Determinations of $[M(CO)_6][SbF_6]_2$ at 300 K (M = Fe,[20] Ru, Os)[a]

	Fe[20]	Ru(11)	Ru(12)	Ru(5)	Os(10)	Os(6)	Os(9)
			(i) Unit Cell Parameters and Dimensions				
$a = b$ (Å)	8.258(1)	8.278(1)	8.284(1)	8.289(1)	8.274(1)	8.273(1)	8.283(1)
c (Å)	12.471(2)	12.449(2)	12.461(2)	12.447(2)	12.421(2)	12.447(2)	12.414(2)
V (Å^3)	850.5(2)	853.1(2)	855.1(2)	855.2(2)	850.3(2)	851.9(2)	851.7(2)
			(ii) Structure Solution				
total data	10466	12506	9307	9252	9094	9327	6796
unique data	545	555	554	547	549	551	555
observed data	405	430	395	454	362	335	287
parameters	39	39	38	38	39	39	39
GOF on F^2	1.03	1.058	1.004	1.121	1.001	1.270	0.941
R1 [$I > 2\sigma(I)$]	0.0259	0.0219	0.0255	0.0286	0.0196	0.0296	0.0311
wR2	0.0668	0.0624	0.0640	0.0794	0.0506	0.0674	0.0538
			(iii) Internuclear Distances (Å)				
M−Cl	1.917(7)	2.020(6)	2.027(6)	2.019(7)	2.013(8)	2.031(10)	2.022(11)
M−C2	1.903(6)	2.026(5)	2.023(6)	2.033(5)	2.026(6)	2.034(10)	2.019(12)
C1−O1	1.097(8)	1.100(8)	1.099(8)	1.106(10)	1.109(11)	1.094(13)	1.090(11)
C2−O2	1.114(7)	1.101(6)	1.108(7)	1.091(6)	1.101(7)	1.091(11)	1.125(12)
Sb−F1	1.851(5)	1.856(2)	1.856(3)	1.858(2)	1.856(2)	1.852(3)	1.859(5)
Sb−F2	1.832(3)	1.843(4)	1.841(5)	1.839(4)	1.840(4)	1.836(6)	1.843(8)
			(iv) Nonbonding Contacts to M (Å)				
M···Sb	5.174(7)	5.179(7)	5.183(7)	5.183(7)	5.173(7)	5.176(7)	5.175(7)
M···F	3.725(7)	3.731(6)	3.735(7)	3.732(6)	3.725(6)	3.732(7)	3.729(9)
			(v) Nonbonding, Interionic Contacts (Å)[b]				
C2···F1	2.842(5)	2.822(5)	2.827(5)	2.822(5)	2.819(5)	2.821(5)	2.816(6)
O2···F1	2.853(5)	2.867(5)	2.876(5)	2.868(5)	2.868(5)	2.873(5)	2.880(6)
C2···F1′	3.062(5)	3.059(5)	3.061(5)	3.057(5)	3.049(5)	3.060(5)	3.056(6)
O2···F1′	3.162(6)	3.203(6)	3.200(6)	3.198(6)	3.193(6)	3.198(6)	3.184(8)
C1···F2	3.339(7)	3.307(7)	3.308(7)	3.313(7)	3.306(7)	3.303(7)	3.305(9)
O1···F2	3.117(6)	3.121(6)	3.124(6)	3.127(6)	3.120(6)	3.121(6)	3.123(8)

[a] For crystal structure details, see Tables 1 and S1 and ref 20. [b] $\sum r_{\text{van der Waals}}$: O···F, 2.99 Å; C···F, 3.13 Å.

and the interionic bonding in the six salts are similar; (ii) to subsequently determine whether structural similarities also extend to relevant spectroscopic (vibrational, ^{13}C NMR) properties; and (iii) to provide a rationale for any observed close correspondences or possibly also differences in experimental data, with assistance from relevant computations, mainly by Jonas and Thiel.[21]

(ii) Crystal Data and Unit Cell Parameters. The data are summarized in Table 1, with a more detailed listing pertaining to the structural solutions as well, found in Tables S1 and S2. For the three $[M(CO)_6][SbF_6]_2$ salts (M = Fe,[20] Ru, Os), the unit cell dimensions are nearly identical. Differences are very slightly larger than the stated error limits. The unit cell of $[Fe(CO)_6][SbF_6]_2$ appears to be more tetragonally elongated along the c axis by about 0.05 Å relative to the Os(II) compound and by about 0.02 Å relative to the Ru(II) compound, whereas a and b are very slightly shorter. However, the unit cell volumes V for $[M(CO)_6][SbF_6]_2$ (M = Fe, Os) are identical within error limits, with that for $[Ru(CO)_6][SbF_6]_2$ being slightly larger by about 0.3%.

The unit cell parameters a, b, c, and β and the volume V are again all very slightly smaller for $[Fe(CO)_6][Sb_2F_{11}]_2$[19] than for the Ru (by ~1.4%) and Os (by ~1.0%) $[Sb_2F_{11}]^-$ salts (see Table 1). In the absence of relativistic effects for the 3d species,[49,50] this is expected, considering the experimental Fe−C distances (see Tables 2 and 3) and the average Fe−C distances listed in the Cambridge data index[90] (Table 4), which are both shorter by about 6%. However, this argument does not appear to apply to $[Fe(CO)_6][SbF_6]_2$,[20] as discussed above.

Additional information pertaining to the crystal data and the molecular structure determinations of the four metal carbonyl fluoroantimonates ($[Sb_2F_{11}]^-$, $[SbF_6]^-$) for M = Ru and Os is presented as Supporting Information. The listings there include atomic coordinates and thermal parameters for $[M(CO)_6][Sb_2F_{11}]_2$ (M = Ru, Os; Tables S3 and S4) and for $[M(CO)_6][SbF_6]_2$ (M = Ru, Os; Tables S5 and S6), the corresponding data for previously reported[20] $[Fe(CO)_6][Sb_2F_{11}]_2$ and $[Fe(CO)_6][SbF_6]_2$ (Tables S7a and S7b), and finally a comparison of atomic coordinates for all three $[M(CO)_6][SbF_6]_2$ salts (M = Fe,[20] Ru, Os) in Table S8.

All data in Tables S1−S8 support the strong similarity of the six salts in the two isostructural triads $[M(CO)_6][Sb_2F_{11}]_2$ and $[M(CO)_6][SbF_6]_2$ (M = Fe,[20] Ru, Os) with respect to crystallographic data (Tables 1 and 2) and atomic coordinates. This similarity is also reflected in the bond parameters, as discussed in the next section.

(iii) Internal Bond Parameters for $[M(CO)_6][Sb_2F_{11}]_2$ and $[M(CO)_6][SbF_6]_2$ (M = Fe,[20] Ru, Os). The internal bond parameters (internuclear distances and bond angles) for both cations and anions of the six isostructrual salts of the compositions $[M(CO)_6][Sb_2F_{11}]_2$ and $[M(CO)_6][SbF_6]_2$ (M = Fe,[20] Ru, Os) are presented in the following manner: A complete listing of internal bond parameters for the new species $[M(CO)_6][Sb_2F_{11}]_2$ and $[M(CO)_6][SbF_6]_2$ (M = Ru, Os)[18] is found in the Supporting Information as Tables S8 and S9.

(90) Orpen, A. G.; Brammer, L.; Allen, F. H.; Kennard, O.; Watson, D. G.; Taylor, R. *J. Chem. Soc., Dalton Trans.* **1989**, Suppl. 1.

Table 3. Experimental and Calculated[21] Internuclear Distances for $[M(CO)_6]^{2+}$ in $[M(CO)_6][Sb_2F_{11}]_2$ (M = Fe,[20] Ru, Os) and Related Species

	Fe[20]		Ru		Os	
(a) M−C and C−O (in Brackets) Distances (Å)						
(i) $[M(CO)_6]^{2+}$						
$d(M-C_1)$ $[d(C_1-O_1)]^a$ ×2	1.911(5)	[1.103(5)]	2.044(9)	[1.086(9)]	2.032(5)	[1.097(6)]
$d(M-C_2)$ $[d(C_2-O_2)]$ ×2	1.912(5)	[1.102(5)]	2.027(9)	[1.093(10)]	2.016(5)	[1.109(6)]
$d(M-C_3)$ $[d(C_3-O_3)]$ ×2	1.910(5)	[1.107(5)]	2.045(8)	[1.100(8)]	2.032(5)	[1.097(6)]
$d(M-C_{avg})$ $[d(C-O)_{avg}]$	1.911(5)	[1.104(5)]	2.039(8)	[1.094(10)]	2.027(6)	[1.102(7)]
$d(M-C'_{avg})$ $[d(C'-O)_{avg}]^b$	1.908(7)	[1.108(7)]	2.024(6)	[1.101(6)]	2.022(7)	[1.104(8)]
(ii) $M(CO)_5$						
$d(M-C_{ax})$ $[d(C-O)$ ×2	1.806(5)	[1.145(4)][20]	1.950(9)	[1.143(3)][66]	1.962(8)	[1.142(4)][67]
$d(M-C_{eq})$ x 3	1.833(4)		1.969(9)			
(b) Statistical[c,d] Data from the Cambridge Index[90]						
$d(M-C)$ $(n)^e$	1.782 (2572)		1.896 (1453)		1.902 (1443)	
(c) Calcualted Data[20]						
$d(M-C)$ $[d(C-O)]$	1.905	[1.130]	2.028	[1.130]	2.045	[1.130]

[a] See Figures 3 and 4 for numbering of atoms. [b] Data obtained for $[M(CO)_6][SbF_6]_2$ (M = Fe,[20] Ru, Os) are collected in Tables 2 and 3. [c] Reference 89. [d] *d* for CO in metal carbonyl compounds is listed as 1.145 Å based on 10022 examples. [e] Number of examples in ref 89.

Table 4. Vibrational Frequencies (cm^{-1}) for the Fundamentals of $[M(CO)_6]^{2+}$ in $[M(CO)_6][SbF_6]_2$ (M = Fe,[20] Ru, Os)

assignments (description)	Fe		Ru		Os	
	obsd[b]	calcd[a]	obsd[b]	calcd[a]	obsd[b]	calcd[a]
ν_1, ν_{CO} (A_{1g})	2242 s	2221	2252 s	2235	2258 s	2237
ν_3, ν_{CO} (E_g)	2219 s	2188	2219 s	2192	2214 vs	2188
ν_6, ν_{CO} (T_{lu})	2205 (70)	2173 (100)	2198 (80)	2172 (100)	2189 (105)	2166 (100)
ν_7, δ_{MCO} (T_{1u})	590 (70)	608 (29)	556 (46)	572 (23)	560 (50)	567 (16)
ν_{12}, δ_{MCO} (T_{2u})	470 (0.1)	478	483 (0.1)	490	509 (0.04)	509
ν_{10}, δ_{MCO} (T_{2g})	500 w	508	463 s	468	480 w	471
ν_2, ν_{MC} (A_{1g})	345 m	361	388 m	401	429 m	428
ν_4, ν_{MC} (E_g)	357 w, sh	355	379 w, sh	377	409 w	401
ν_8, ν_{MC} (T_{1u})	382 (<0.1)	380 (3)	335 (7)	337 (5)	344 (9)	336 (8)
ν_5, δ_{MCO} (T_{1g})	331[c]	338	328[c]	329	345[c]	339
n_9, g_{CMC} (T_{1u})	148[c]	117 (0.3)	146[c]	106 (0.1)	145[c]	101 (0.0)
ν_{11}, δ_{CMC} (T_{2g})	148 vs	98	139 vs	91	142 vs	93
ν_{13}, δ_{CMC} (T_{2u})	94[c]	77	92[c]	75	96[c]	77

[a] BP86/ECP2.[21] Relative IR intensities in parentheses, where 100 denotes approximately 1035 (Fe), 1260 (Ru), and 1545 (Os) km/mol. [b] Relative IR intensities in parentheses normalized to the strongest anion band (ν_{SbF}, T_{1u}, denoted as 100). For Raman intensities, s = strong, m = medium, w = weak, v = very, sh = shoulder. [c] Calculated from combination bands. Estimated uncertainty: ν_5, ±2; ν_9 and ν_{13}, +5 cm^{-1}.

Selected bond parameters for $[M(CO)_6][SbF_6]_2$ (M = Fe,[20] Ru, Os) are compiled in Table 2, and in Table 3, experimental internuclear C−O and M−C distances for the $[M(CO)_6]^{2+}$ cations (M = Fe,[20] Ru, Os) in the triad $[M(CO)_6][Sb_2F_{11}]_2$ are summarized and compared to the corresponding experimental data for the molecular species $M(CO)_5$, obtained by electron diffraction,[20,66,67] and statistical data for M−CO complexes (M = Fe, Ru, Os) from the Cambridge data index.[90]

To emphasize the nearly identical internal bond parameters for the three members in both triads (see Tables 2, 3, S9, and S10), a generic pictorial presentation is chosen: formula units of $[M(CO)_6][Sb_2F_{11}]_2$ and $[M(CO)_6][SbF_6]_2$ (M = Fe,[20] Ru, Os) are shown in Figures 3 and 4, respectively, to introduce the numbering used in this study for both cations and anions. To emphasize their electrophilic nature, the carbonyl C atoms[9−12,21] are highlighted in both figures.

Finally, in Figure 5, important parameters of the dioctahedral $[Sb_2F_{11}]^-$ anions in the three $[M(CO)_6][Sb_2F_{11}]_2$ salts (M = Fe,[20] Ru, Os) are shown in a schematic representation that concentrates on the skeletal bridging moiety and omits the terminal F_{eq} atoms in both SbF_4 groups. As can be seen, the conformation of all three $[Sb_2F_{11}]^-$ anions is C_1. The diagnostic criteria, first introduced by Holloway et al.;[91] the bridge angles α; and the dihedral angles ψ in all three

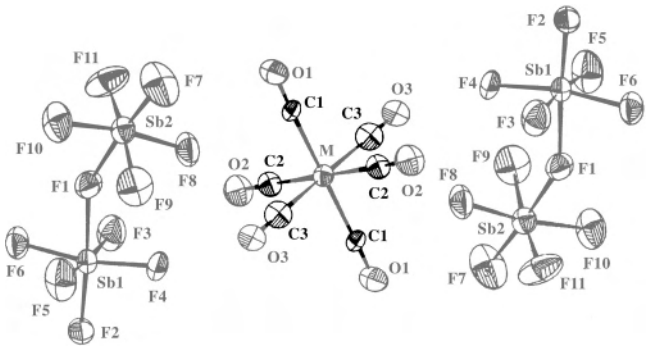

Figure 3. Molecular structure of $[M(CO)_6][Sb_2F_{11}]_2$: Formula unit; 50% probability ellipsoids; M = Fe,[20] Ru, Os.

symmetry-related anions are identical within error limits. Also identical is the asymmetry within the $Sb_1-F_b-Sb_2$ bridges and all six $Sb-F_{ax}$ bond lengths, whereas for all three $[M(CO)_6][Sb_2F_{11}]_2$ salts (M = Fe,[20] Ru, Os), the observed $Sb-F_{eq}$ distances for the two planar SbF_4 groups fall into very similar, narrow ranges.

The strong similarities in bond parameters for all three $[Sb_2F_{11}]^-$ anions extend also to the $[SbF_6]^-$ anions for the second triad of the type $[M(CO)_6][SbF_6]_2$ (M = Fe,[20] Ru,

(91) Bruce, D. M.; Holloway, J. H.; Russell, D. R. *J. Chem. Soc., Dalton Trans.* **1978**, 64.

Table 5. Observed Band Positions and Estimated Intensities[a] for Vibrational Bands (cm^{-1}) Due to $[SbF_6]^-$ of $[M(CO)_6][SbF_6]_2$ (M = Fe,[20] Ru, Os)

assignments and description	Fe[20]		Ru		Os	
	IR	Raman	IR	Raman	IR	Raman
$\nu_4 + 2\nu_6$	683 (0.3) sh		680 (0.3) sh		681 (0.3) sh	
$\nu_3(T_{1u})\ \nu_{SbF}$	665 (100)		663 (100)		663 (100)	
$\nu_1(A_{1g})\ \nu_{SbF}$		652 (30)		651 (30)		652 (30)
$2\nu_4$		590 (1.1) sh		588 (1.0) sh		590 (0.9) sh
$\nu_4 + \nu_5$			581 (0.2)		584 (0.3)	
$\nu_2(E_g)\ \nu_{SbF}$	570 (5.0)	570 (4.0)	*b*	570 (3.9)	*b*	571 (3.2)
$\nu_4(T_{1u})\ \delta_{FSbF}$	292 (60)	291 (2.4)	291 (57)	292 (2.6) sh	291 (60)	292 (3.1) sh
$\nu_5(T_{2g})\ \delta_{FSbF}$	282 sh	281 (11)	281 sh	281 (11)	281 sh	281 (13)

[a] Relative intensities for anion and cation are bands obtained by setting IR action $\nu_{SbF}(T_{1u})$ as 100 and $\nu_{SbF}(A_{1g})$ as 30 in the Raman spectra. [b] Expected band for $\nu_2(E_g)$ coincides with $\nu_7\ \delta_{MCO}(T_{1u})$ for $[M(CO)_6]^{2+}$ (M = Fe, Ru, Os).

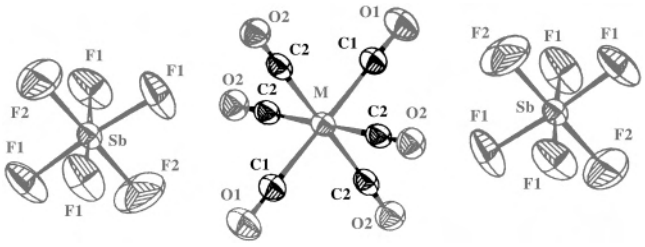

Figure 4. Molecular structure of $[M(CO)_6][Sb_2F_{11}]_2$: Formula unit; 50% probability ellipsoids; M = Fe,[20] Ru, Os.

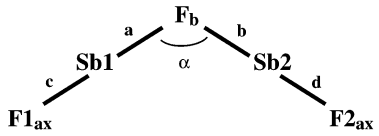

M	Bridge Angle α [°]	Dihedral Angle Ψ [°]	Bridge Distance a [Å]	Bridge Distance b [Å]	Distance Sb1-F_{ax} c [Å]	Distance Sb2-F_{ax} d [Å]	Range of dSb-F_{eq} [Å]
Fe[20]	148.5(2)	38	2.053(3)	1.998(3)	1.850(3)	1.836(4)	1.810(3)-1.869(3)
Ru	148.5(3)	38	2.052(5)	2.003(5)	1.847(5)	1.837(6)	1.804(7)-1.869(5)
Os	148.1(3)	38	2.054(4)	2.001(5)	1.847(3)	1.844(6)	1.829(5)-1.871(4)

Figure 5. Skeletal moiety of the $[Sb_2F_{11}]^-$ anion (point group C_1; F_{eq} omitted) and diagnostic structural parameters of the $[Sb_2F_{11}]^-$ anions in the three salts $[M(CO)_6][Sb_2F_{11}]^-$ (M = Fe,[20] Ru, Os). In all three salts, the two $[Sb_2F_{11}]^-$ units have identical bond parameters.

Os). The anions are again symmetry-related and depart from O_h symmetry by a small tetragonal distortion (compression) as a consequence of the tetragonal space group (vide supra). This is evident from the Sb−F bond lengths listed in Tables 2 and S9. Approximately octahedral symmetry is also evident from a vibrational analysis of the $[SbF_6]^-$ anion in all three salts, shown in Table 5, as discussed more fully below.

Tetragonal distortion (elongation) is evident also for the $[M(CO)_6]^{2+}$ cations in the triad $[M(CO)_6][SbF_6]_2$ (M = Fe,[20] Ru, Os), but as for the $[SbF_6]^-$ anions, tetragonal distortions are more pronounced for $[Fe(CO)_6][SbF_6]_2$,[20] just as the unit cell parameters for the three salts had suggested. For $[M(CO)_6][SbF_6]_2$ (M = Ru, Os), both the M−C distances (M = Ru, Os) and the observed tetragonal distortions are within the stated error limits (see Tables 2, 3, S9, and S10).

Likewise, the M−C and C−O distances, with the latter less pronounced, in the triad $[M(CO)_6][Sb_2F_{11}]_2$ (M = Fe,[20] Ru, Os) show trigonal distortions as a consequence of the monoclinic crystal system (see Table 1). The trigonal distortions are more noticeable for the Ru and Os salts, but the M−C distances in the two compounds are identical within error limits.

When average M−C distances (M = Fe,[20] Ru, Os) are considered as well (see Table 3), two simple conclusions are reached: (i) M−CO bonding in octahedral $[M(CO)_6]^{2+}$ (M = Fe,[20] Ru, Os) is of identical strength regardless of counteranion. (ii) In both triads, $[M(CO)_6]^{2+}$ cations are completely isostructural for M = Ru and Os, which is neither predicted[21] nor evident from statistical data, compiled in the Cambridge data collection, where slightly longer Os−CO bonds are suggested.[21,90] For both $[Fe(CO)_6]^{2+}$ salts,[20] experimental as well as calculated[21] and statistical[90] Fe−CO bonds are shorter than the corresponding Ru−CO and Os−CO internuclear distances.

As is commonly found for σ-bonded metal carbonyl cations,[9−20,42−44,58] C−O bond lengths for all six[9−17,20,42−44,58] salts in both $[M(CO)_6]^{2+}$ triads (M = Fe,[20] Ru, Os) are, consistent with calculations,[21] among the shortest compiled in the Cambridge index,[90] regardless of metal (Fe, Ru, or Os) or counteranion ($[Sb_2F_{11}]^-$ or $[SbF_6]^-$). However, at high C−O bond orders, experimental internuclear C−O distances are all identical within error limits (see Table 3), and vibrational data [ν(CO), f_{CO}] provide a much more accurate estimate of C−O bond strength (Tables 4 and 6, and Figures 6 and 7), as discussed below.

In addition to the internal bond parameter discussed above, significant interionic contacts are observed in fluoroantimonate salts of superelectrophilic σ-bonded metal carbonyls[8−19,42−45] and their derivatives. Their importance in the six $[M(CO)_6]^{2+}$ salts (M = Fe,[20] Ru, Os) is now analyzed.

(iv) Inter- and Intraionic Interactions in $[M(CO)_6][Sb_2F_{11}]_2$ and $[M(CO)_6][SbF_6]_2$ (M = Fe,[20] Ru, Os). The strong similarities of the observed internal bond parameters of the $[M(CO)_6]^{2+}$ cations (M = Fe,[20] Ru, Os; Tables 2 and 3) and the octahedral $[SbF_6]^-$ anions (Tables 2, 3, and 5) and the identical conformations as well as all diagnostic bond parameters of the $[Sb_2F_{11}]^-$ anions (Figure 5) in all six salts discussed here allow the conclusion that secondary[92] interionic contacts must be similar in both number and strength for the three salts in each triad.

In particular, the data for the three $[Sb_2F_{11}]^-$ anions, summarized in Figure 5, are supportive of this view. We have previously argued, based on a substantial body of evidence from structural studies,[10−16,20,42−45] that the dioc-

(92) Alcock, N. W. *Adv. Inorg. Chem. Radiochem.* **1972**, *15*, 1.

Table 6. Summary of Selected Experimental and Calculated Structural and Spectroscopic Parameters of the Superelectrophilic, Octahedral Cations $[M(CO)_6]^{2+}$ (M = Fe, Ru, Os)

	Fe[20]		Ru		Os	
	(a) Solid-State Complex Anion					
	$[SbF_6]^-$	$[Sb_2F_{11}]^-$	$[SbF_6]^-$	$[Sb_2F_{11}]^-$	$[SbF_6]^-$	$[Sb_2F_{11}]^-$
$\nu(CO)_{avg}$ (cm^{-1})	2216	2215	2214	2216	2209	2211
$f_{CO} \times 10^2$ ($N \cdot m^{-1}$)	19.83	19.82	19.80	19.83	19.71	19.75
$d(C-O)_{avg}$ (Å)	1.108(7)	1.104(5)	1.101(6)	1.094(10)	1.104(8)	1.102(7)
$d(M-O)_{avg}$ (Å)	1.908(7)	1.911(5)	2.024(6)	2.039(8)	2.022(7)	2.027(6)
$\nu(M-C)_{avg}$ (cm^{-1})	368	368	359	362	382	384
	(b) ^{13}C NMR data for $[M(CO_6)]^{2+}$(solv)					
$\delta^{13}C$ (ppm)	178		168.8		150.6	
$J(^{13}C-M)$ (Hz)	19.2		60.8		91.7	
	(c) Calculated Data[21] for $[M(CO)_6)]^{2+}$(g)					
$\nu(CO)_{avg}$ (cm^{-1})	2185		2189		2185	
$F_{CO} \times 10^2$ ($N \cdot m^{-1}$)	19.20		19.22		19.13	
$d(CO)$ (Å)	1.130		1.130		1.130	
$d(M-C)$ (Å)	1.905		2.028		2.045	
$f_{M-C} \times 10^2$ ($N \cdot m^{-1}$)	1.77		1.89		2.16	
q_c (e^-)[a]	0.63		0.63		0.60	
q_M (e^-)[a]	−0.49		−0.51		−0.35	
q_O (e^-)[a]	−0.21		−0.21		−0.21	

[a] Partial atomic charges from natural population analysis.[20]

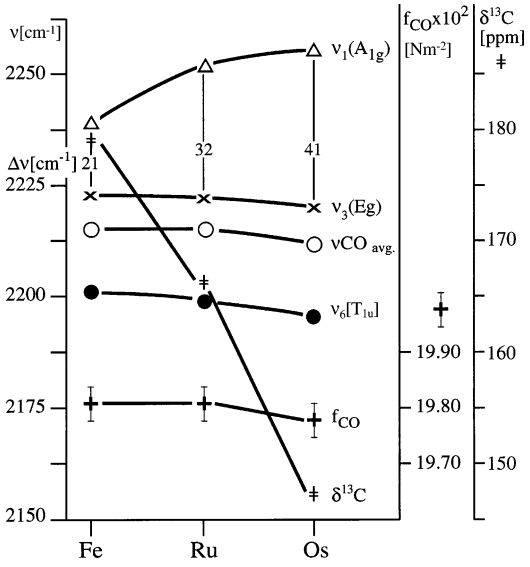

Figure 6. Fundamental CO stretching frequencies and ^{13}C chemical shifts for $[M(CO)_6]^{2+}$ (M = Fe,[20] Ru,[18] Os)[18].

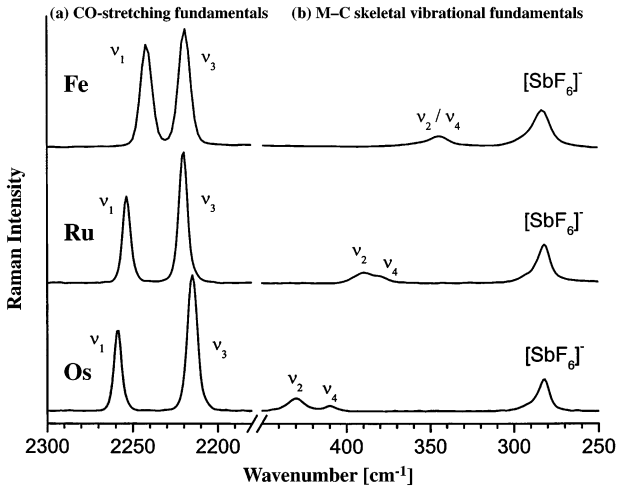

Figure 7. Raman spectra of $[M(CO)_6][SbF_6]_2$ (M = Fe,[20] Ru, Os).

Table 7. Selected Bonding and Nonbonding Contacts[a] (Å) for C_n (n = 1, 2, 3)[b] in the Structures of $[M(CO)_6][SbF_6]_2$ and $[M(CO)_6][Sb_2F_{11}]_2$ (M = Fe,[20] Ru, Os)

	bonding		nonbonding	
compound	$d(M-C1)$	$d(C1-O)$	$d(C1\cdots C2/3)$	$d(C1/3\cdots F)$
$[Fe(CO)_6][SbF_6]_2$	1.917	1.097	2.701	2.842
$[Fe(CO)_6][Sb_2F_{11}]_2$	1.911	1.103	2.684−2.723	2.718−2.969
$[Ru(CO)_6][SbF_6]_2$	2.020	1.100	2.865	2.822
$[Ru(CO)_6][Sb_2F_{11}]_2$	2.044	1.086	2.862−2.896	2.724−2.909
$[Os(CO)_6][SbF_6]_2$	2.013	1.109	2.856	2.819
$[Os(CO)_6][Sb_2F_{11}]_2$	2.031	1.099	2.831−2.893	2.741−2.903

[a] Uncorrected data listed without estimated standard deviations. [b] See Figures 3 and 4 for numbering of atoms.

tahedral $[Sb_2F_{11}]^-$ anion in salts with superelectrophilic[8] metal carbonyl cations[10−12] will distort by bending at the F bridge (expressed in terms of the bridge angle α) and by rotation of the two SbF_4 moieties (resulting in a dihedral angle Ψ)[11,91] from an ideal D_{4h}[93] symmetry, to facilitate the formation of significant and numerous interionic C···F contacts. The strength of these contacts is judged by comparison to the sums of the corresponding van der Waals nonbonding radii, tabulated by Bondi.[94]

In salts of σ-bonded metalcarbonyl cations with fluoroantimonate anions,[9−12] the sums of van der Waals radii of 3.17 and 2.99 Å for C···F and O···F contacts, respectively, are viewed as upper limits. For the purpose of illustration, in $[Hg(CO)_2][Sb_2F_{11}]_2$[44] and $[M(CO)_4][Sb_2F_{11}]_2$ (M = Pd, Pt[43]) with linear[44] or square-planar[43] metal carbonyl cations, up to five significant C···F contacts for each C atom are observed with contact distances as short as 2.6 Å[43,44]

As seen in Figures S1 and S2 in the Supporting Information and in Tables 2 and 7, for salts with octahedral $[M(CO)_6]^{2+}$ cations (M = Fe,[20] Ru, Os), far fewer and weaker interionic C···F contacts are observed: In $[M(CO)_6][Sb_2F_{11}]_2$ (M = Fe,[20] Ru, Os), only one significant C···F contact per CO ligand is found with the shortest contact distance of 2.724 Å, whereas in $[M(CO)_6][SbF_6]_2$, four

(93) Sham, I. H. T.; Patrick, B. O.; Thompson, R. C.; Aubke, F.; von Ahsen, B.; von Ahsen, S.; Willner, H. *Solid State Sci.* **2002**, *4*, 1457.
(94) Bondi, A. *J. Phys. Chem.* **1964**, *68*, 441.

C···F contacts per $[M(CO)_6]^{2+}$ cation (M = Fe,[20] Ru, Os) are detected, with distances between 2.818 and 2.842 Å. In both triads, the strength of these interionic interactions appears to increase slightly from the Fe to the Os complex. Slightly shorter contact distances for the $[Sb_2F_{11}]^-$ salts reflect the nonrigidity of the dioctahedral anions.[11,91]

In both $[M(CO)_6]^{2+}$ triads (M = Fe,[20] Ru, Os), the reduced accessibility of the carbonyl C atoms by F atoms of the anions in the strictly octahedral cations provides a plausible explanation for fewer and weaker C···F interactions, compared to findings for $[M(CO)_4][Sb_2F_{11}]_2$ (M = Pd, Pt[43]) or $[Hg(CO)_2][Sb_2F_{11}]_2$.[44] Alternatively, it can be argued that octahedral $[M(CO)_6]^{2+}$ cations (M = Fe,[20] Ru, Os) are intrinsically more stable than are square-planar $[M(CO)_4]^{2+}$ (M = Pd, Pt) or linear $[Hg(CO)_2]^{2+}$ ions, which are stabilized only by $[Sb_2F_{11}]^-$ and not by $[SbF_6]^-$.[43,44] This view is reflected in the reported thermal stabilities, which, in the 5d series, follow the order $[Hg(CO)_2][Sb_2F_{11}]_2$ (160 °C)[44] < $[Pt(CO)_4][Sb_2F_{11}]_2$ (230 °C)[43] < $[Os(CO)_6][SbF_6]_2$ (350 °C), with decomposition points in parentheses.[10,11]

As seen in Table 2, for the three $[M(CO)_6][SbF_6]_2$ salts (M = Fe,[20] Ru, Os), in addition to weak C2···F contacts, there are equally weak O2···F interactions, which are slightly shorter than 2.99 Å, the sum of the van der Waals radii for O and F.[94] This observation is in harmony with a bonding model for fluoroantimonate salts with σ-bonded metal carbonyl cations proposed recently.[10−12] According to this model, electron transfer from F atoms of the fluoroanimonate anions into π^* MOs of the CO ligands becomes a competing process to d(M) → π^* back-donation in a classical synergic bonding view.[98,99] With M in oxidation states of 2+ or 3+,[10−12] σ donation from CO to M^{n+} is augmented by increased polarization of the CO bond by M^{n+}, $n = 2,3$.[51]

A vibrational analysis of octahedral homoleptic metal carbonyls of W^0, Re^+, Os^{2+}, and Ir^{3+} [10−13] has provided a spectroscopic basis for the bonding model. Additional support for the proposed F → π^* interionic back-donation comes from the observed M−C−O bond angles, which, in most instances, depart from linearity by ∼2−3° [10−16,42−44] This is also the case for $[Fe(CO)_6][Sb_2F_{11}]_2$[20] and $[M(CO)_6][Sb_2F_{11}]_2$ (M = Ru, Os; see Tables S8 and S9) However, in $[M(CO)_6][SbF_6]_2$ (M = Fe,[20] Ru, Os), the observed M−C1−O angles (M = Fe,[20] Ru, Os) are strictly linear, whereas for M-C2-O (M = Fe,[20] Ru, Os), the departures are small, ∼1° or less (Tables S10 and S11), because the $[SbF_6]^-$ ion appears to be less effective in F → π^* back-donation than $[Sb_2F_{11}]^-$, as stated above.

In addition to the observed interionic C···F and O···F interactions (listed in Tables 2 and 7), there are nonbonding C···C contacts within the three $[M(CO)_6]^{2+}$ cations (M = Fe,[20] Ru, Os), which are also listed in Table 7. The observed contacts for the six salts are significantly shorter than the sum of the van der Waals radii of 3.40 Å[94] and reflect the tight packing of electrophilic C atoms[21] in the octahedral coordination spheres of the $[M(CO)_6]^{2+}$ cations (M = Fe,[20] Ru, Os). For the Ru and Os cations, these C···C contacts are similar in both cations and show a slight dependency on the counteranion ($[SbF_6]^-$ or $[Sb_2F_{11}]^-$). Shorter C···C contacts suggesting tighter packing of the C atoms is found for both $[Fe(CO)_6]^{2+}$ salts[20] with very slight dependency on the counteranion. An illustration of the tight packing in $[M(CO)_6]^{2+}$ (M = Fe,[20] Ru, Os) is found in Figure S7.

The structural data for $[M(CO)_6][SbF_6]_2$ (M = Fe,[20] Ru, Os) compiled in Table 2 provide a summary and good overview of the structure and bonding situation for $[Ru(CO)_6][SbF_6]_2$ and $[Os(CO)_6][SbF_6]_2$. Three different crystals of each salt were chosen in each case. Their structures were solved identically, with full details of the structure solution included. The unit cell dimensions and relevant internuclear distances were obtained for all six crystals, and the results were compared to the corresponding published data for $[Fe(CO)_6][SbF_6]_2$.[20] Also included were nonbonding (M···Sb, M···F) distances and secondary interionic (C···F, O···F) contacts, which were compared to the relevant sums of the van der Waals radii.[94]

As can be seen, the unit cell dimensions, internuclear distances, and various nonbonding contacts for $[Ru(CO)_6][SbF_6]_2$ and $[Os(CO)_6][SbF_6]_2$ are extremely close. Differences between the two data sets are often smaller than variations found for the three crystals of the same metal. Although internuclear Fe−C distances in $[Fe(CO)_6][SbF_6]_2$[20] are shorter than those for the Ru and Os compounds, interionic bonding is weaker, reflected in slightly longer C···F contacts than are found for $[M(CO)_6][SbF_6]_2$ (M = Ru, Os). As a consequence, in the triad $[M(CO)_6][SbF_6]_2$ (M = Fe,[20] Ru, Os), the unit cell dimensions and volumes, nonbonding M···Sb and M···F distances (M = Fe, Ru, Os), and Sb−F bond lengths are all independent of the metal.

These findings together with other crystallographic and bonding details, such as the identical conformations and bonding parameters for the $[Sb_2F_{11}]^-$ anions, shown in Figure 5, make the six compounds studied here unique and the results obtained unprecedented among structurally characterized metal carbonyl cations and their derivatives.[9−17,42−44]

(v) Structure and Bonding in the Triads $[M(CO)_6][Sb_2F_{11}]_2$ and $[M(CO)_6][SbF_6]_2$ (M = Fe,[20] Ru, Os): A Summary. Bond parameters for the $[Sb_2F_{11}]^-$ and $[SbF_6]^-$ salts are identical in the two triads, as are the conformations and diagnostic bond parameters for $[Sb_2F_{11}]^-$ in $[M(CO)_6][Sb_2F_{11}]_2$ (M = Fe,[20] Ru, Os). Bond parameters for $[M(CO)_6]^{2+}$ (M = Ru, Os) are nearly independent of M in both triads on account of relativistic effects.[49,50] Slightly shorter Fe−C bonds[20] are partially compensated by stronger interionic contacts for the corresponding ruthenium and osmium compounds, so that unit cell dimensions are independent of the metal in the triad $[M(CO)_6][SbF_6]_2$ (M = Fe,[20] Ru, Os) and very similar for the three $[Sb_2F_{11}]^-$ salts. It appears that crystal packing of $[SbF_6]^-$ ions in the lattice is tighter and more efficient than that of dioctahedral $[Sb_2F_{11}]^-$ anions.

(95) Jones, L. H.; McDowell, R. S.; Goldblatt, M. *Inorg. Chem.* **1988**, *27*, 2349.
(96) Abel, E. W.; McLean, R. A. N.; Tyfield, S. P.; Braterman, P. S.; Walker, A. P.; Hendra, P. J. *J. Mol. Spectrosc.* **1969**, *30*, 29.
(97) Cotton, F. A.; Kraihanzel, C. S. *J. Am. Chem. Soc.* **1962**, *84*, 4432.
(98) Dewar, J. S. *Bull. Soc. Chim. Fr.* **1951**, *18*, C71.
(99) Chatt, J.; Duncanson, L. A. *J. Chem. Soc.* **1953**, 2939.

An additional controlling factor that affects the size of the $[M(CO)_6]^{2+}$ cations (M = Fe,[20] Ru, Os) is repulsive interactions between the C atoms of the six carbonyl ligands (see Figure S7 and Table 7), which, according to a natural population analysis,[21] have nearly identical positive partial charges (see Table 6 and ref 21).

In harmony with the results of the DSC study reported here, M−C bond strength appears to increase from Fe to Ru to Os in the cation $[M(CO)_6]^{2+}$ (M = Fe, Ru, Os) because of increased C−O bond polarization and relativistic effects.[49,50]

A similar trend of increasing bond strength for the C−O bonds in the three cations is expected but not found (see Figure 4), as the subsequent discussion of the vibrational spectra shows, because F → π^* external electron delocalization[10−12] will follow the order Fe < Ru ≤ Os. In this respect, $[Sb_2F_{11}]^-$ is found to be a slightly more effective donor of electron density than $[SbF_6]^-$. This is reflected in the crystallographic data reported here, as well as in the case of many more $[Sb_2F_{11}]^-$ salts with superelectrophilic metal carbonyl cations.[9−17,20,42−45]

Although the members of the two triads $[M(CO)_6][Sb_2F_{11}]_2$ and $[M(CO)_6][SbF_6]_2$ (M = Fe, Ru, Os) are isostructural and the counteranions $[Sb_2F_{11}]^-$ and $[SbF_6]^-$ have identical bond parameters and conformations, a careful analysis brings to light subtle but fascinating differences as well as similarities that are unique in metal carbonyl chemistry.[1−7,9−12,75]

(c) Vibrational Spectra of $[M(CO)_6][SbF_6]_2$ (M = Fe,[20] Ru, Os). Although the crystal and molecular structures of $[M(CO)_6][Sb_2F_{11}]_2$ and $[M(CO)_6][SbF_6]_2$ (M = Ru, Os) are reported here for the first time, the initial report on the synthesis of $[M(CO)_6][Sb_2F_{11}]_2$ (M = Ru, Os[18]) contains a preliminary vibrational assignment for the $[M(CO)_6]^{2+}$ cations (M = Ru, Os). An early review[9] compares vibrational spectra of the isoelectronic octahedral species $W(CO)_6$,[95] $[Re(CO)_6]^+$,[96] $[Os(CO)_6]^{2+}$,[18] and $[Ir(CO)_6]^{3+}$ [15] in the ν(CO) range. A second horizontal correlation of the same four $M(CO)_6$ species (M = W, Re^+, Os^{2+}, Ir^{3+}) contains a complete vibrational analysis of $[Os(CO)_6]^{2+}$ and $[Ir(CO)_6]^{3+}$ [13] (Figure S5) in conjunction with the structural characterization of $[Ir(CO)_6][SbF_6]_3$·4HF. An extensive DFT study[21] of octahedral $M(CO)_6$ species includes a complete vibrational assignment and calculated band positions and intensities of IR bands for $[M(CO)_6]^{2+}$(g) (M = Fe, Ru, Os), and other theoretical studies[22−24] report more limited vibrational frequencies in the ν(CO) range. All of these earlier experimental studies[9,13,15] and the DFT calculations of Jonas and Thiel[21] establish a strong similarity of the vibrational spectra, at least in the CO stretching range, between $[M(CO)_6]^{2+}$ (M = Ru, Os) and $[Fe(CO)_6]^{2+}$. The latter has been extensively characterized with both $[Sb_2F_{11}]^-$ and $[SbF_6]^-$ as counteranions by ^{13}C substitution, normal coordinate analysis (NCA), and force constant (GVFF) calculations.[20]

In the course of this study,[20] it was found that $[Fe(CO)_6][SbF_6]_2$ is more suitable for a vibrational analysis than the $[Sb_2F_{11}]^-$ salt, on account of the much simpler vibrational spectrum of octahedral $[SbF_6]^-$, which results in less band overlap. In addition, Raman spectra are more informative, whereas IR spectra of crystalline samples are occasionally ambiguous, on account of the Christiansen effect, other artifacts, and interference from combination bands.

Hence, to avoid unnecessary duplication and redundancy, the following approach is taken here: (i) Rather than providing a complete vibrational analysis of $[M(CO)_6]^{2+}$ (M = Ru, Os), the data obtained by us are compared to experimental results for $[Fe(CO)_6]^{2+}$ [20] and to previously reported calculated data[21] for $[M(CO)_6]^{2+}$(g) (M = Fe, Ru, Os). (ii) Earlier studies on $[M(CO)_6]^{2+}$ (M = Fe, Ru, Os)[9,13,18,20] limited to the ν(CO) range, are summarized in the form of a diagram, shown in Figure 6. Also listed here are $\nu(CO)_{avg}$, f_{CO},[97] and ^{13}C chemical shifts (discussed later). (iii) A complete list of vibrational fundamentals for $[M(CO)_6]^{2+}$ (M = Fe,[20] Ru, Os) is provided in Table 4. Experimental frequencies are compared to calculated values.[21] (iv) The Raman spectra of $[M(CO)_6]^{2+}$ (M = Fe,[20] Ru, Os) in the $[SbF_6]^-$ salts are shown in Figure 7, and the fundamentals for $[SbF_6]^-$ in all three salts are listed in Table 5. (v) A complete listing of all IR-active vibrations including overtones for $[M(CO)_6][SbF_6]_2$ (M = Fe,[20] Ru, Os) together with an assignment are available as Supporting Information in Table S11. (vi) Vibrational spectra of $[Ru(CO)_6][SbF_6]_2$ and $[Os(CO)_6][SbF_6]_2$ are shown as Supporting Information in Figures S3 and S4.

As reported for $[Fe(CO)_6]^{2+}$,[20] the band positions of all 13 fundamentals have been obtained experimentally also for the $[M(CO)_6]^{2+}$ cations (M = Ru, Os; see Table 4) with the band positions of ν_5 (T_{1g}), ν_9 (T_{1u}), and ν_{12} (T_{2u}) estimated from combination bands. The inactive vibration ν_{12} (T_{2u}) is observed as a very weak band in the IR spectra.

The assignment of the vibrational spectra for $[Ru(CO)_6]^{2+}$ and $[Os(CO)_6]^{2+}$ is obtained in a similar manner as described for $[Fe(CO)_6]^{2+}$ in greater detail. Support comes from the calculated[20] (BP86/ECP2) band positions and IR intensities. As discussed previously,[20] calculated band positions for the CO stretching modes ν_1, ν_3, and ν_6 are underestimated,[20] as is ν[CO(g)] itself,[21] pointing to a limitation of the DFT method. Values for ν_9, ν_{11}, and ν_{13} are also somewhat higher than calculated frequencies, presumably because of crystal lattice effects. For the remaining fundamentals, only minor discrepancies between experimental and calculated band positions are noted.

Just as reported for both $[Fe(CO)_6]^{2+}$ salts[20] and suggested by the structural data discussed above, vibrational data for all $[M(CO)_6]^{2+}$ cations (M = Fe,[20] Ru, Os) are independent of the counteranion $[Sb_2F_{11}]^-$ or $[SbF_6]^-$. This is convincingly illustrated by a comparison of the CO stretching fundamentals ν_1, ν_3, and ν_6 for $[M(CO)]_6][Sb_2F_{11}]_2$[18,20] (M = Fe, Ru, Os), plotted in Figure 6, to the corresponding values for the same three fundamentals for $[M(CO)_6][SbF_6]_2$ (M = Fe,[20] Ru, Os) listed in Table 6. Differences in band positions are at most 4 cm^{-1} and fall for the most part within error limits.

The reasonably close similarities of calculated[21] and experimentally observed fundamentals of $[M(CO)_6]^{2+}$ (M = Fe, Ru, Os[18−20]) and the noted independence of the coun-

teranion ($[Sb_2F_{11}]^-$ or $[SbF_6]^-$), best documented in the CO stretching fundamentals (Figures 6 and 7, Table 4), together with the limited number of rather weak interionic contacts in all six $[M(CO)_6]^{2+}$ salts (M = Fe,[20] Ru, Os), are all indications of the exceptional intrinsic stability of the octahedrally coordinated, homoleptic, superelectrophilic,[8] σ-bonded metal carbonyl cations[9−12] in group 8.

The same conclusions can be extended to superelectrophilic[8] $[Ir(CO)_6]^{3+}$, where all fundamentals[13,15,19] compare well to calculated values and where identical band positions are found in the CO stretching region in $[Ir(CO)_6]^{3+}$(solv), HF/SbF_5,[13] $[Ir(CO)_6][Sb_2F_{11}]_3$,[15,19] and $[Ir(CO)_6][SbF_6]_3 \cdot 4HF$.[13]

Due to increased π-back donation in the series $[M(CO)_6]^{2+}$ (M = Fe,[20] Ru, Os), there is a slight dependence of vibrational band positions most noticeable in the C−O and M−C stretching regions, on the central metal ion M^{2+} (M = Fe,[20] Ru, Os), which appears to affect the three fundamentals ν_1 (A_{1g}), ν_3 (E_g), and ν_6 (T_{1u}) differently. In the CO stretching region (see Figures 6 and 7 and Table 4), the A_{1g} mode increases gradually in the triad $[M(CO)_6]^{2+}$ from Fe[20] to Ru to Os by 10 and 6 cm^{-1}, respectively. The E_g mode ν_3 changes very little, and for Ru and Os, a decrease of 5 cm^{-1} is noted. Finally, for ν_6 (T_{1u}), a gradual decrease by 7 and 9 cm^{-1} is noticed. As a consequence of these changes in opposite directions, $\nu(CO)_{avg}$ and f_{CO} are nearly identical for $[Fe(CO)_6]^{2+}$ and $[Ru(CO)_6]^{2+}$ and only slightly smaller for $[Os(CO)_6]^{2+}$ (see Table 7). For the skeletal M−C stretching fundamentals, a similar, more pronounced trend emerges. However, in this far more cluttered spectral region, vibrational assignments can occasionally be ambiguous, and vibrational coupling or "mixing" is a strong possibility. Hence, some caution is advised.

As seen in Figure 7, in the Raman spectra, the band positions for ν(MC) of ν_2 (A_{1g}) and ν_4 (E_g) shift strongly from Fe to Os to higher frequencies, and the peak separation increases. As seen in Table 4, the observed shifts of ν_2 are 43 and 41 cm^{-1} and those of ν_4 are 22 and 30 cm^{-1}, with band separations of 12, 9, and 20 cm^{-1}, respectively, for the two fundamentals in $[M(CO)_6]^{2+}$ in the order Fe[20] < Ru < Os. There is good agreement between experimental and calculated[21] frequencies in this region as discussed above.

The trend of ν_8 (T_{1u}) in the IR spectra is less clear, because there is both, a dependence of the metal atom mass and force constant.

Nevertheless, a simple interpretation is possible: The strength of the M−C bond and, to a less noticeable degree, of the C−O bond in the $[M(CO)_6]^{2+}$ cations increases in the order of Fe[20] < Ru < Os. As the covalent character of the M−C bond increases, the band separations between ν_1 and ν_3 and between ν_2 and ν_4 increase, as seen in Figure 7. Support comes from the thermal stabilities of $[M(CO)_6][SbF_6]_2$ (M = Fe, Ru, Os), studied by DSC, discussed in the first part of this publication and from DFT calculations of f_{M-C}, included in Table 6.

A previously reported horizontal correlation for isoelectronic, octahedral $[M(CO)_6]$ complexes with M = W, Re^+, Os^{2+}, and Ir^{3+} in the 5d series was used to generate a plot of the CO stretching fundamentals versus the nuclear charge for the four complexes, as shown in Figure S5. The increased frequencies for all three fundamentals, in particular for ν_1 (A_{1g}), are affected by electron delocalization from F into the π^* MOs of the CO ligands,[10−13] which increases with increasing oxidation state of M, M = Re^+, Os^{2+} Ir^{3+}. In addition to an increase in ν(CO), the band separation for the three fundamentals decreases with increasing oxidation state of M.[9,13,95,96]

The intensities of the CO stretching fundamentals have been discussed before.[9] In all instances, in the Raman spectra, ν_1 (A_{1g}) is of lower intensity than ν_3 (E_g),[9−12,18,95,96] and only for $[Ir(CO)_6]^{3+}$ [9,13,20] the two fundamentals do have identical intensities.

Finally, consistent with their strong structural similarities (see Tables 2 and 3), discussed above, the fundamentals of $[SbF_6]^-$ in $[M(CO)_6][SbF_6]_2$ (M = Fe,[20] Ru, Os) have identical band positions in all three salts as shown in Table 5.

(d) ^{13}C NMR Spectra of $[M(CO)_6]^{2+}$ (M = Fe, Ru, Os). The solubilities of the $[M(CO)_6][SbF_6]_2$ salts (M = Fe, Ru, Os) in HF are sufficiently high that their ^{13}C NMR spectra can be recorded. In addition to the ^{13}C resonance, in all cases, we are able to detect satellite resonances, produced by ^1J (^{13}C−M) coupling with an NMR-active metal nucleus (see Table S12).

The rather rare case of coupling to a nucleus with a spin of $^5/_2$ for ^1J (^{13}C−^{99}Ru) is shown in Figure S6. All six satellite resonances are detected. The line widths of the satellites are, at 2 Hz, significantly broader than is observed in the case of ^1J (^{13}C−^{57}Fe) or ^1J (^{13}C−^{187}Os) on account of the quadrupole moment of ^{99}Ru. Coupling with ^{101}Ru ($s = ^5/_2$, abundance 17.1%) is not observed, on account of its much higher quadrupole moment (0.44). The same explanation is valid for ^{189}Os ($s = ^3/_2$, abundance 16.1%, $Q = 0.8 \times 10^{-24}$ cm^2). The observed ^{13}C NMR parameters are reported in Table 6.

In the triad Fe, Ru, Os, the chemical shifts decrease down the group, and at the same time, the reduced coupling constants increase. A similar trend of chemical shifts is obtained in DFT calculations.[23] The larger change in J between Ru and Os compared to the change between Fe and Ru is seen to be due mainly to relativistic effects.[49,50] A more detailed analysis will also involve the pairs $[M(CO)_4]^{2+}$ (M = Pd, Pt),[43] $[M(CO)_5Cl]^{2+}$ (M = Rh, Ir),[14] and $[Hg(CO)_2]^{2+}$.[44]

Summary and Conclusions

With the conjugate Brønsted−Lewis superacid HF/SbF_5[35−41] as the reaction medium, two divergent synthetic approaches, reductive carbonylation[9−12,18,19] of $M(SO_3F)_3$ (M = Ru, Os)[29−31] or OsF_6 and oxidative carbonylation of $Fe(CO)_5$[54] with XeF_2 as the oxidizer,[20] allow the syntheses of two isostructural triads: $[M(CO)_6][Sb_2F_{11}]_2$ and $[M(CO)_6][SbF_6]_2$ (M = Fe,[20] Ru, Os).[18,19] A previously reported rationale for reductive carbonylation[11,12] is now extended to the oxidative carbonylation of $Fe(CO)_5$[20,54] (Scheme 1).

The compounds of the composition $[M(CO)_6][SbF_6]_2$ show thermal stabilities that range from 180 °C (M = Fe) to 350

°C (M = Os) before CO evolution occurs, according to a DSC study (see Figure 2), supplemented by a gas-phase IR analysis of volatile products.

As seen in Table 1, the members in each triad $[M(CO)_6][Sb_2F_{11}]_2$ (monoclinic, $P2_1/n$; Figure 3) and $[M(CO)_6][SbF_6]_2$ (tetragonal, $P4/mnc$; Figure 4) are isostructural; have very similar unit cell parameters, including unit cell volumes and identical bond parameters for the anions, $[Sb_2F_{11}]^-$ (see Figure 2) and $[SbF_6]^-$ (Tables 2 and 3), and have vibrational properties (Table 4) that are invariant of M.

The structural properties of the $[M(CO)_6]^{2+}$ (M = Fe,[20] Ru, Os) are independent of the counteranion. Very similar, slightly shorter Fe−C internuclear distances (Tables 2 and 3) are partly compensated by stronger interionic M···C contacts for M = Ru, Os (Table 4), resulting in similar sizes of the cations, apparent from the listed nonbonding C···C contacts in the octahedral coordination spheres (Table 7).

Dependence of spectroscopic properties on the metal is found for (i) ^{13}C NMR data, summarized in Table 6 and illustrated in Figure 6; (ii) M−C skeletal vibrations, listed in Table 4 and shown in Figure 7; and (iii) small shifts in the CO stretching range (see Figure 7 and Table 4). Trends in ν(CO) and ν(MC) suggest increased bond strength of the M−C bond and covalency in $[M(CO)_6]^{2+}$ (M = Fe, Ru, Os) with increased nuclear charge of M.

The principal experimental and calculated[21] structural and spectroscopic properties of the intrinsically stable, octahedral $[M(CO)_6]^{2+}$ cations (M = Fe,[20] Ru, Os) are summarized in Table 6.

The results reported here allow the conclusion that the octahedral $[M(CO)_6]^{2+}$ cations (M = Fe, Ru, Os) should also be generated in other Brønsted−Lewis superacids[35,36] and stabilized by counteranions other than the fluoroantimonates, which have been used exclusively so far.[9−16,18−20,42−46] As a first result in this direction, the synthesis and structural characterization of $[M(CO)_6][BF_4]_2$ (M = Fe, Ru, Os)[100] is reported as part 2 of this study.

Acknowledgment. Financial support by Deutsche Forschungsgemeinschaft, Fonds der Chemischen Industrie, Natural Sciences and Engineering Research Council of Canada, North Atlantic Treaty Organization, and Alexander v. Humboldt Foundation is gratefully acknowledged. We are indebted to Ms. M. Litz (Universität Wuppertal) for typing the manuscript, Ms. S. Harbour (UBC) for editing and Ms. E. Varty (UBC) for illustrations. Degussa-Hüls is thanked for the gift of Ru and Os powders.

Supporting Information Available: Detailed crystallographic data, information on structure solution, atomic coordinates and thermal parameter, bond distances and bond angles, listings of the vibrational bands, structural drawings and figures of the vibrational spectra for $[M(CO)_6][Sb_2F_{11}]_2$ and $[M(CO)_6][SbF_6]_2$ (M = Ru, Os), and X-ray crystallographic files. This material is available free of charge via the Internet at http://pubs.acs.org.

IC040115U

(100) Finze, M.; Bernhardt, E.; Willner, H.; Lehmann, C. W.; Aubke, F. *Inorg. Chem.* **2005**, *44*, 4206−4214.